Geologica Acta, Vol. 11, Nº 2, June 2013, 177-193
DOI: 10.1344/105.000001779
Available online at www.geologica-acta.com

geologica acta

The Bartonian-Priabonian marine record of the eastern South Pyrenean foreland basin (NE Spain): a new calibration of the larger foraminifers and calcareous nannofossil biozonation

E. COSTA [1, 4] **M. GARCÉS** [1, 4] **M. LÓPEZ-BLANCO** [1, 4] **J. SERRA-KIEL** [1, 4]
G. BERNAOLA [2] **L. CABRERA** [1, 4] **E. BEAMUD** [3, 4]

[1] **Departament d'Estratigrafia, Paleontologia i Geociències Marines, Facultat de Geologia, Universitat de Barcelona (UB)**
C/ Martí i Franquès s/n, 08028-Barcelona, Spain. Costa E-mail: elicosta@ub.edu Garcés E-mail: mgarces@ub.edu
López-Blanco E-mail: m.lopezblanco@ub.edu Serra-Kiel E-mail: josepserra@ub.edu Cabrera E-mail: lluis.cabrera@ub.edu

[2] **Departamento de Ingeniería Minera y Metalúrgica y Ciencia de los Materiales. EUIT de Minas y Obras Públicas. UPV/EHU**
Colina de Beurko s/n, 48902-Barakaldo, Spain. Bernaola E-mail: gilen.bernaola@ehu.es

[3] **Laboratori de Paleomagnetisme UB-CSIC. Centres Científics i Tecnològics UB (CCiTUB). Institut de Ciències de la Terra "Jaume Almera" (CSIC)**
C/ Solé i Sabarís s/n, 08028-Barcelona, Spain. Beamud E-mail: betbeamud@ub.edu

[4] **Institut GEOMODELS. Grup de recerca consolidat Geodinàmica i Anàlisi de Conques (GGAC)**
Barcelona Knowledge Campus

ABSTRACT

This study presents a combined biostratigraphic (calcareous nannofossils, larger foraminifers) and magnetostratigraphic study of the Middle and Late Eocene marine units of the Igualada area, eastern Ebro Basin. The studied sections of Santa Maria de Miralles and La Tossa encompass the complete marine succession of the Santa Maria Group, where assemblages rich in larger foraminifers have been studied since the early 1950's. A total of 224 paleomagnetic sites and 62 biostratigraphic samples were collected along a 1350m-thick section that ranges from chron C20n to chron C16n (~43Ma to ~36Ma). The resulting magnetostratigraphy-based chronology challenges existing chronostratigraphic interpretations of these units and results in a new calibration of the biostratigraphic zonations. The base of calcareous nannofossil Zone NP19-20 is pinned down to an older age than its presently accepted attribution, whereas the time span assigned to Zone NP18 is significantly reduced. A revised calibration of larger foraminifers indicates that Zone SBZ18, formerly assigned exclusively to the late Bartonian, extends its range to the earlymost Priabonian, the Bartonian stage being almost entirely represented by Zone SBZ17. A division of Zone SBZ18 into two subzones is proposed.

KEYWORDS | **Middle/Late Eocene. Chronostratigraphy. Magnetostratigraphy. Biostratigraphy. Time Scale.**

INTRODUCTION

Providing a robust high-resolution chronostratigraphic scheme of the geological record is essential for the advance of earth-science research (Gradstein *et al.*, 2004). Age control is the key to calculate rates of change in geodynamic systems and to unravel cause-effect relationships. Magnetostratigraphy has been successfully proved to constitute an effective dating tool of stratigraphic successions (Langereis *et al.*, 2010), capable of integrating disparate records on a global basis. In combination with biostratigraphic methods, it provides the means for increasing resolution of the geological time scale (Langereis *et al.*, 2010; Agnini *et al.*, 2011).

The South Pyrenean foreland basin (NE Spain) has for long awaked the curiosity of geologists because of its exceptional sedimentary record (Virgili, 2007). The present level of erosion of the basin infill and its surrounding mountain ranges is at an optimal stage for studying tectonostratigraphic relationships on surface, making this region a natural laboratory for the study of collision belts and their adjacent foreland systems. A biochronological framework of the South Pyrenean foreland basin has been developed since the early 1950's (Ruiz de Gaona and Colom, 1950; Ruiz de Gaona, 1952; Hottinger, 1960; Hottinger and Schaub, 1960; Reguant, 1967; Colom, 1971; Ferrer, 1971a, b; Kapellos and Schaub, 1973; Caus, 1973, 1975; Schaub, 1981; Serra-Kiel, 1984; Tosquella, 1995; Papazzoni and Sirotti, 1995; Romero *et al.*, 1999; Romero, 2001; Hottinger *et al.*, 2001), which was later combined with magnetostratigraphic studies (Burbank *et al.*, 1992a). All the available literature on the biostratigraphy and magnetostratigraphy of the Paleocene and Eocene Tethys were integrated in a general chronostratigraphic framework, used to define and calibrate the larger foraminifer biozonation (Shallow Benthic Zones, SBZ) (Serra-Kiel *et al.*, 1998a, b).

A recent study has challenged the Middle-Late Eocene chronostratigraphy of the South Pyrenean foreland basin, showing that the youngest marine deposits in the Vic region, of presumed Bartonian age, yield calcareous nannofossils assigned to the Priabonian Zone NP19-20 (Cascella and Dinarès-Turell, 2009). Furthermore, a magnetostratigraphic study focused on the overlying continental units of the Artés Formation (Costa *et al.*, 2010) confirmed these results, dating the marine-continental transition in the Ebro Basin within chron C16n (*i.e.* Priabonian).

In this paper we present a new integrated biomagnetostratigraphic study of the Eocene marine units in the Igualada area, close to the SE margin of the South Pyrenean foreland basin. The results provide a revised chronology of

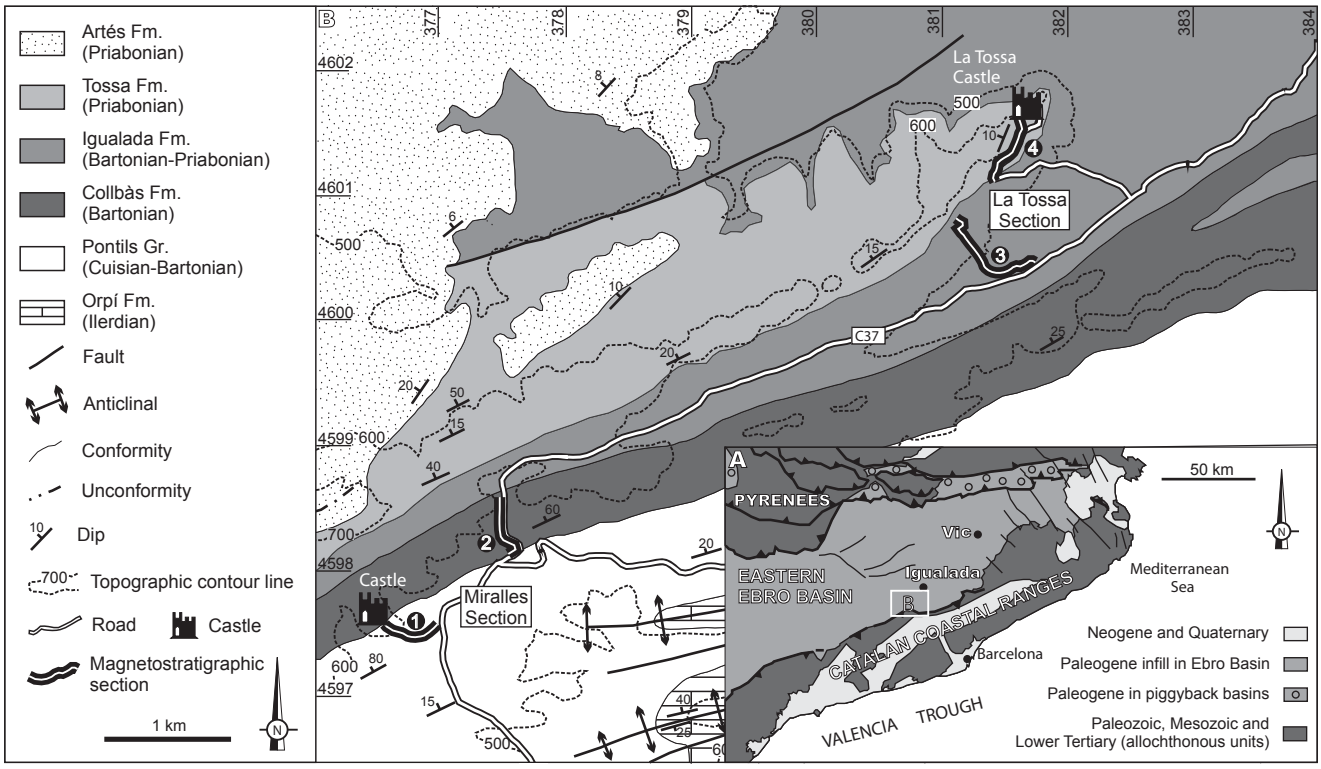

FIGURE 1 | Geological setting of the Miralles and La Tossa sections. A) Main geological units in the NE Iberian Peninsula. B) Detailed geological map of the study area with indication of the Miralles (1 and 2) and La Tossa (3 and 4) sections. Map coordinates are in UTM projection, ED50/zone 31N.

these stratigraphic units, and a new calibration of the Late Eocene marine standard biozonation.

GEOLOGICAL SETTING

The present geology of NE Iberia has resulted from two successive plate-tectonic scenarios. First, the Late Cretaceous to Miocene convergence and continental collision between the Iberian and Eurasian plates (Anadón and Roca, 1996), which led to the growth of the Pyrenean thrust belt at the plate boundary, and the formation of the South Pyrenean foreland basin on the subducting Iberian Plate (Zoetemeijer *et al.*, 1990; Muñoz, 1992; Beaumont *et al.*, 2000; Vergés *et al.*, 2002). Second, the Oligocene-Miocene rift and opening of the western Mediterranean Basin and related extension of the eastern Iberian margin (Roca *et al.*, 1999).

The South Pyrenean foreland basin (Fig. 1) is filled with up to 5000 meters of marine and continental sediments ranging in age from Upper Cretaceous to Middle Miocene. Marine deposition was dominant along its northern margin, where subsidence was greater (Riba *et al.*, 1983). Paleogeographic reconstructions for the Middle-Late Eocene (Meulenkamp and Sissingh, 2003) show that the South Pyrenean region formed a narrow marine corridor connecting the Atlantinc and Tethyan oceanic domains. No precise constraint exists on the age of closure of its eastern gateway, presumably taking place during the Bartonian (Plaziat, 1981; Meulenkamp and Sissingh, 2003; Serra-Kiel *et al.*, 2003a), leading the basin to evolve into an elongated gulf, only connected with oceanic waters through the Bay of Biscay. Marine sedimentation in the foreland basin ended in the Priabonian (Costa *et al.*, 2010), after the tectonic uplift and closure of its western marine gateway.

The latest evolutionary stage of the South Pyrenean foreland basin, namely the Ebro Basin (Riba *et al.*, 1983), is bounded to the SE and SW by the Catalan Coastal Ranges and the Iberian Chain, respectively. In addition to the South-Pyrenean foredeep, the eastern margin of the Ebro Basin also developed a secondary foredeep zone as a consequence of thrusting and uplift of the Catalan Coastal Range from the Early Eocene until the Late Oligocene (Guimerà, 1984; Anadón *et al.*, 1985a). In the central sector of the Catalan Coastal Ranges, maximum deformation occurred in the Middle-Late Eocene, as recorded by the syntectonic development of alluvial-fan and fan-delta systems (López-Blanco, 2002). In the eastern Ebro Basin, two important transgressive events of Ilerdian and Bartonian age are recognized. Following the basin closure, steady and continuous continental sedimentation took place from Late Eocene to the late Middle Miocene (Barberà *et al.*, 2001; Pérez-Rivarés *et al.*, 2002), rising the basin base level to nearly one thousand meters above sea level. Alluvial and fluvial sedimentation predominated in the basin margins (Anadón *et al.*, 1985a; López-Blanco *et al.*, 2000; López-Blanco, 2002); whereas in the inner parts fluvial and lacustrine systems were set up (Anadón *et al.*, 1989; Cuevas *et al.*, 2010).

The end of sedimentation in the Ebro Basin (Middle-Late Miocene) occurred as a combined result of basin overfilling and escarpment erosion across the differentially rifted and uplifted Catalan margin (García-Castellanos *et al.*, 2003; Urgelés *et al.*, 2011). River incision allied with rift shoulder uplift and accelerated erosion of both the central Catalan Coastal Ranges and the eastern Ebro Basin (Gaspar-Escribano *et al.*, 2004), bringing to surface the complete basin infill sequence with a smooth northwestward tilt.

STRATIGRAPHY OF THE MIDDLE-UPPER EOCENE RECORD OF THE EASTERN EBRO BASIN

The Middle-Upper Eocene record of the SE margin of the South Pyrenean foreland basin in the Igualada area consists of a 2000m-thick transgressive-regressive sequence divided into three units (Figs. 2; I.1 Electronic Appendix available at www.geologica-acta.com): a lower continental unit (Pontils Group), a middle marine unit (including the Santa Maria Group, the "Terminal Complex" and the Cardona Formation), and an upper continental succession (Artés Formation). All these three units laterally grade towards the margin into alluvial conglomeratic units such as the Montserrat, Sant Llorenç del Munt, and Montclar conglomerates.

The Pontils Group (Ferrer, 1971a; Anadón, 1978) consists of red mudstones with interbedded carbonatic and evaporitic sediments deposited in continental and transitional environments. These sediments were first attributed to Cuisian and Lutetian ages as determined by charophyte assemblages (Rosell *et al.*, 1966; Ferrer, 1971a). They were subsequently attributed to the Lutetian and Bartonian according to the proposed charophyte biozonation of Anadón and Feist (1981) and Anadón *et al.* (1992).

The marine sediments of the Santa Maria Group (Ferrer, 1971a), comprise three main formations; the Collbàs Formation (limestone and marl levels with subordinated sandstones and fine conglomerates corresponding to the nearshore deposits), the offshore marls of the Igualada Formation, and the Tossa Formation, a coralline limestone unit that corresponds to reef and bioclastic bar environments. On top of these sediments the shallow water carbonate platforms of the "Terminal Complex" (Travé,

1992; Travé *et al*., 1996; Fig. I.1), the halite-dominated Cardona Formation and its sulfate-dominated evaporitic Òdena and La Noguera formations (Pueyo, 1974) represent the uppermost marine sediments deposited in the Ebro Basin.

Two transgressive-regressive cycles were earlier described in the Middle-Upper Eocene marine deposits of the Igualada area (Serra-Kiel *et al*., 2003b). The first sedimentary cycle corresponds to the Collbàs Formation, and its maximum flooding surface is determined at the transition from marls with larger foraminifers and ahermatypical corals to marls. The second sedimentary cycle includes the rest of the marine deposits of the Igualada area (Igualada and Tossa formations, the "Terminal Complex" and the Cardona Formation) and its maximum flooding surface is represented by a marker level that covers the Igualada area and has been interpreted as a condensation level, containing abundant *Discocyclina*, *Asterocyclina*, *Assilina* and *Operculina*.

The pioneering studies in the Middle-Upper Eocene marine record of the eastern Ebro Basin made the attempt to apply the Paris Basin chronology by ascribing Auversian, Bartonian and/or Ledian ages to the marine Santa Maria Group (Ruiz de Gaona and Colom, 1950; Ruiz de Gaona, 1952). However, the description of two new stages (Ilerdian and Biarritzian) in the Eocene of the western Pyrenees by Hottinger and Schaub (1960) favored the adoption of these chronological units in later works (Rosell *et al*., 1966; Reguant, 1967; Ferrer, 1971a; Caus, 1975; Schaub, 1981; Serra-Kiel, 1984). Subsequently, with a planktonic foraminiferal and a larger foraminiferal biozonation, Ferrer (1971a) established a Biarritzian age (*Truncarotaloides rohri*, *Nummulites perforatus* and *Alveolina elongata* Biozones) to the Collbàs Formation and the lower part of the Igualada Formation. Ferrer (1971b) also attributed a Lower Priabonian age (*Globigerinatheka semiinvoluta* and *Nummulites prefabianii* Biozones) to the upper parts of the Igualada Formation and to the Tossa Formation because of the presence of the larger foraminifers *Pellatispira madaraszi* HANTKEN, 1875 and *Heterostegina reticulata* RÜTIMEYER, 1850 (=*Grzybowskia reticulate*). These results were challenged by Serra-Kiel *et al*. (1998a, b), who used the associations of larger foraminifers of the Igualada area, together with data from other alpine-belt regions, as the basis for the definition of the zones SBZ17 and SBZ18. Currently accepted calibration of the larger foraminiferal biostratigraphy indicates that zones SBZ17 and SBZ18 correlate with the Bartonian stage (Serra-Kiel *et al*., 1998a, b), in accordance with the occurrence of younger SBZ19 assemblages in the Priabonian type locality (Luciani *et al*., 2002).

Laterally equivalent to the uppermost marine sediments and also overlying the top marine beds, the Artés Formation (Ferrer, 1971a), consists of alluvial red beds with interbedded lacustrine limestone units. The basal members of the Artés Formation have yielded scarce biostratigraphic information, reporting Late Eocene to Early Oligocene vertebrate fossil assemblages (Agustí *et al*., 1987; Anadón *et al*., 1987, 1992; Sáez, 1987; Arbiol and Sáez, 1988).

A number of magnetostratigraphic studies spanning the Middle-Upper Eocene record of the eastern Ebro Basin

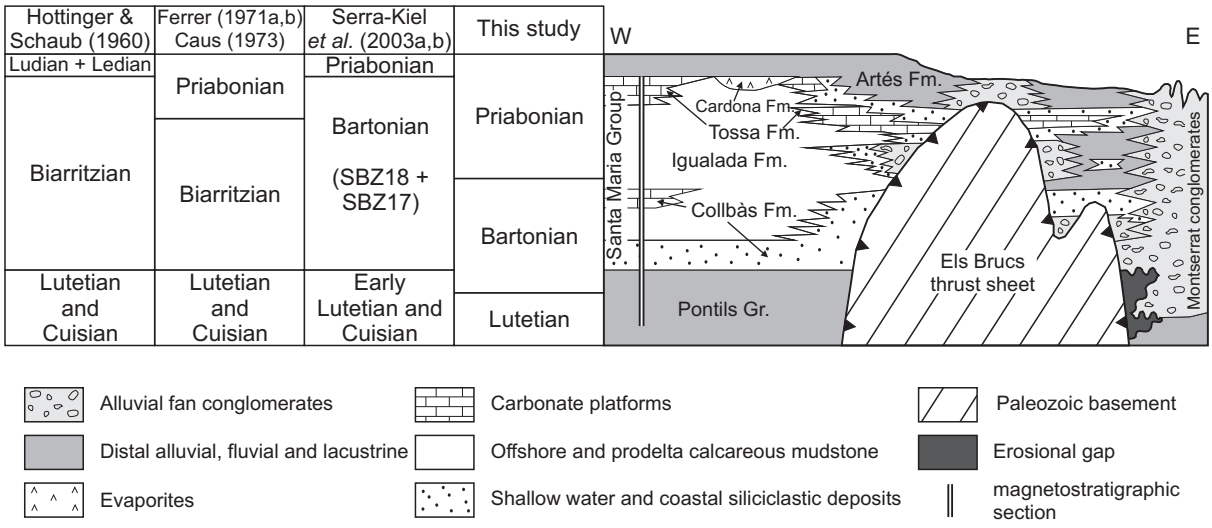

FIGURE 2 | Litho- and biochronostratigraphy of the Igualada area. The lithostratigraphic sketch has no vertical scale and it has been modified from Anadón *et al.* (1985b). Previous biochronostratigraphic information comes from Hottinger and Schaub (1960), Ferrer (1971a, b), Caus (1973) and Sierra-Kiel *et al.* (2003a, b).

were performed in the Vic and Oliana areas during the 1990's (Burbank *et al.*, 1992a, b; Vergés and Burbank, 1996; Taberner *et al.*, 1999). These studies were unable to provide an independent match with the Geomagnetic Polarity Time Scale (GPTS) based on the magnetostratigraphic pattern. On the contrary, their correlations were built on the presumed "Bartonian" age of the foraminiferal assemblages of the top marine units. Recent studies, however, have challenged this view showing the presence of fossil assemblages of Priabonian age in the upper units of the Santa Maria Group (Cascella and Dinarès-Turell, 2009), in agreement with earlier findings of Ferrer (1971b). In support of this scenario, a recent magnetostratigraphic study has independently shown that the marine-continental transition took place in the chron C16n.2n, during the Priabonian (Costa *et al.*, 2010).

NEW DATA FROM THE MIRALLES-LA TOSSA COMPOSITE SECTION

Two stratigraphic sections, spanning the Middle-Upper Eocene record of the Igualada area were sampled for magnetostratigraphy and biostratigraphy (Fig. 1B). The Miralles section (1 and 2 in Fig. 1B) covers the continental sediments of the Pontils Group and the marine Collbàs Formation of the Santa Maria Group. The La Tossa section (3 and 4 in Fig. 1B) covers the Igualada and Tossa formations and has its top in the La Tossa de Montbui castle, 4km south of Igualada. At the top of the La Tossa section and above the patch reef facies that constitutes the Tossa Formation, yellowish marine sandstones occur. These transitional sandstones are a lateral equivalent to the "Terminal Complex" and the Òdena Gypsum Formation (sulfate belt of the halite-dominated Cardona Formation) and constitute the uppermost marine deposits of the South Pyrenean foreland basin (Fig. 2). Correlation between the Miralles and La Tossa sections yields a total thickness of 1350 meters, which includes a non-outcropping stratigraphic gap of 100 meters at the base of the Igualada Formation.

Larger foraminifers

Recorded assemblages

Along the Miralles-La Tossa composite section, 14 samples were collected for the study of larger foraminifers, 9 samples in the Collbàs Formation, 4 samples in the Igualada Formation, and 1 sample in the Tossa Formation (Fig. 3). In addition, 3 samples were collected from the "Terminal Complex" outcropping in Puig Aguilera (Fig. I.1). All the samples were studied by means of isolated specimens, which allowed us to observe the external characters as well as to obtain equatorial and axial sections. The samples from the "Terminal Complex" of the Puig Aguilera were studied in thin section.

Detailed remarks regarding the biostratigraphic content of all samples, and their correspondence to type localities can be found in the "Recorded assemblages" section of the Electronic Appendix.

Larger foraminifers from the Miralles-La Tossa composite section were well described and illustrated by previous authors (*e.g.* Hottinger, 1960; Schaub, 1981; Papazzoni and Sirotti, 1995; Romero *et al.*, 1999; Romero, 2001; Hottinger *et al.*, 2001; Serra-Kiel *et al.*, 2003a). However, some forms such as *Nummulites chavannesi*, *N. garnieri sturi* and *N.* aff. *incrassatus ramondiformis* of the Tossa Formation needed a more accurate description. With that purpose a "Systematic Remarks" section has been added at the Electronic Appendix.

Biostratigraphy

From the study of the Miralles-La Tossa composite section a larger foraminiferal biozonation can be established. The Zone SBZ17 is represented by the occurrence of *Alveolina fragilis*, *Nummulites biarritzensis*, *N. perforatus*, *N. beaumonti*, *N. hottingeri* and *N. praegarnieri* in the interval covering from sample BM005 to sample MM022 (meters 446 to 660), within the Collbàs Formation (Fig. 3). The first occurrence of *N. vicaryi* in sample MM024 (meter 680) and *N. striatus* in sample MM028-029 (meter ~707) indicates the bottom of the Zone SBZ18. The top of this zone is not recognized because of the absence of the typical Zone SBZ19 forms such as *N. fabianii*, *N. cunialensis* and *N. garnieri garnieri*. Noticeable, however, is the occurrence of *Nummulites stellatus* (samples LT000 at meter 825 and LT104 at meter 901.4, Fig. 3) and *Nummulites chavannesi* (sample LT005 at meter 1237.5, Fig. 3), forms of Priabonian age according to Roveda (1961) and Herb and Hekel (1975).

Special attention should be given to the fossil assemblage of sample LT005 (meter 1237.5), which contains *Nummulites* aff. *incrassatus ramondiformis*, *N. garnieri sturi* and *N. chavannesi* (Figs. 3; I.6; I.7; I.8). This assemblage was characterized by Papazzoni and Sirotti (1995) as *Nummulites variolarius/incrassatus* Biozone, and it was considered to be located close to the Bartonian-Priabonian boundary. Characteristic of this interval is the first occurrence of *Pellatispira madaraszi*, *Biplanispira absurda* and *Heterostegina reticulata*, and the absence of *N. striatus*, *N. vicaryi*, *N. boulangeri* and *N. cyrenaicus*. In Figure 3, this zone has been denoted as larger foraminiferal Zone SBZ18b and it comprises the entire Tossa Formation.

Calcareous nannofossils

Recorded assemblages

For the calcareous nannofossil analysis 47 samples were studied from the marine units of the Miralles-La Tossa composite section, 12 from the Collbàs Formation, 25 from the Igualada Formation and 10 from the Tossa Formation (Fig. 3). All the samples were processed following the micropipette method of Bown (1998) and studied under a Leica petrographic microscope at 1500 and 2000 magnification. For the quantitative analysis, at least

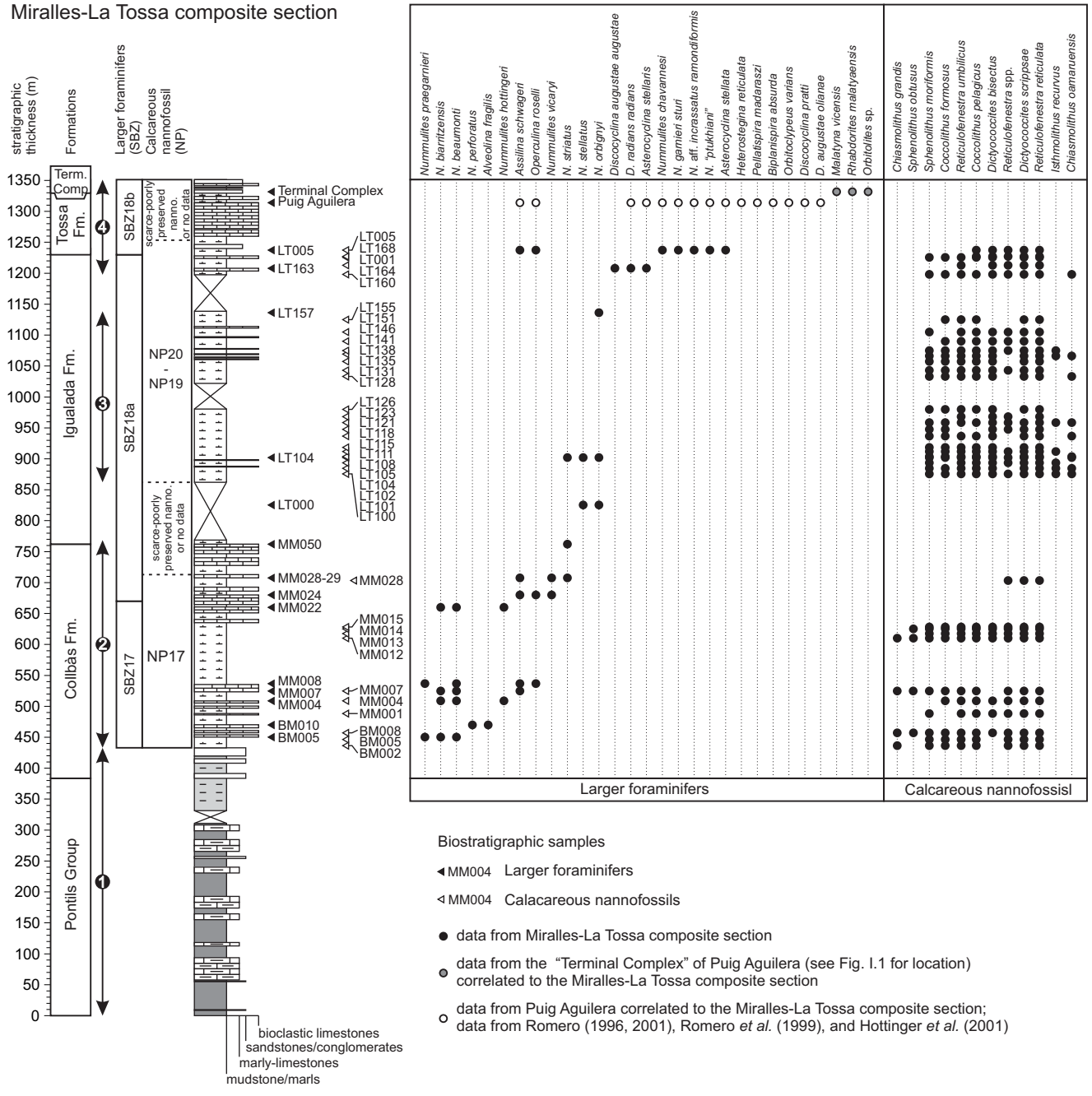

FIGURE 3 Biostratigraphy of the Miralles-La Tossa composite section (larger foraminifers and calcareous nannofossils). Detailed list of the larger foraminifers and their correspondence to type localities of Miralles-La Tossa composite section and Puig Aguilera are provided in the Electronic Appendix available at www.geologica-acta.com. Only the most significant calcareous nannofossil species have been plotted in the figure, for a complete list see Table II. Larger foraminiferal zonation in the Miralles-La Tossa composite section is based on Serra-Kiel *et al.* (1998a), modified. Calcareous nannofossil zonation is from Martini (1791). 1 to 4 correspond to subsections shown in Figure 1B.

300 specimens per sample were counted in a randomly selected field of view. In order to detect rare species with key biostratigraphic value, additional 8mm^2 were analyzed in each sample. The results of the quantitative analysis, summarized in Table II include the preservation degree of the assemblage, the presence of reworked assemblages, the total species abundance (in number of specimens per field of view) and the relative abundance of single species (%).

The total abundance and preservation of calcareous nannofossil assemblages varies along the section. At the base of the Collbàs Formation the reworked Cretaceous species are abundant and the preservation and abundance of autochthonous species is poor. Further up in the succession, the total abundance of calcareous nannofossils increases and the preservation changes from poor to moderate-good. At the upper 50 meters of the Collbàs Formation autochthonous species are almost absent and their preservation is very poor, making impossible the assignment of a calcareous nannofossil zone to this stratigraphic interval. In the lowest samples of the Igualada Formation calcareous nannofossils are again abundant and well preserved. However, from sample LT141 (meter 1074.5) upward, the total abundance decreases distinctly and preservation gets worse. From sample LT155 (meter 1124.7) up to the top of the Igualada Formation, very rare and poorly preserved autochthonous calcareous nannofossils have been recorded. Finally, calcareous nannofossils are absent at the Tossa Formation.

In the Miralles-La Tossa composite section, calcareous nannofossil diversity is relatively low (about 15 species per sample), especially when compared to that registered in the Lower and Middle Eocene of classical Pyrenean sections, such as the Zumaia or Gorrondatxe sections (Orue-Etxebarria *et al.*, 2004; Bernaola *et al.*, 2006). Throughout the Collbàs Formation the assemblage is dominated by *Reticulofenestra reticulata*, *Dictyococcites scrippsae*, *Reticulofenestra umbilicus* and to a lesser extent *Coccolithus pelagicus* and *Coccolithus formosus*. At the Igualada Formation, the calcareous nannofossil assemblage is mainly defined by the same species that dominate the Collbàs Formation with the exception of *Dictyococcites bisectus* that changes from being rare at the base of the Collbàs Formation to being abundant in the Igualada Formation. *Discoaster*, *Sphenolithus* and *Chiasmolithus* are scarce throughout the whole section.

Biostratigraphy and main bioevents

Following the standard biostratigraphic zonation of Martini (1971) the studied interval spans from the upper part of Zone NP17 to the undifferentiated Zone NP19-NP20 (Fig. 3). Zones NP19 and NP20 are combined because the First Appearance Datum (FAD) of *Sphenolithus pseudoradians*, the marker of the base of Zone NP20, is an unreliable marker (Aubry, 1983; Gradstein *et al.*, 2004). The Zone NP18, defined by the stratigraphic interval between the FAD of *Chiasmolithus oamaruensis* and the FAD of *Isthmolithus recurvus*, has not been recorded at the Miralles-La Tossa composite section. In the present study these two biomarkers first occur together from the lowermost sample of the Igualada Formation. The lack of record of Zone NP18 in this study could be due to the almost absence and very poor preservation of calcareous nannofossils in the upper 50 meters of the Collbàs Formation and the non-outcropping 100m-thick interval at the base of the Igualada Formation.

Calcareous nannofossil biostratigraphy of the Miralles-La Tossa section allows recognition of 6 relevant bioevents (Fig. 3) as described below.

First occurrences of *Dictyococcites scrippsae* and *Dictyococcites bisectus*. *D. scrippsae* has been recorded from the lowermost sample of the studied interval whereas *D. bisectus* has its first occurrence in sample BM008 (meter 457.5). The first occurrence of *D. bisectus* is not easy to pinpoint precisely in this section since it is rare in the lower part of its range and the preservation of the calcareous nannofossil assemblages in the lower portion of the Collbàs Formation is poor. The first occurrences of *D. scrippsae* and *D. bisectus* have been used by many authors to mark the base and middle part of NP17 respectively. However, recent studies carried out at Ocean Drilling Program (ODP) Legs 198 (Shatsky Rise, Pacific Ocean), ODP Site 1052 (Blake Nose, northwestern Atlantic Ocean), Agost section (southeastern Spain), and Alano section (northern Italy) show that the first occurrence of both species occur earlier in zones NP15 and NP16 (Bralower, 2005; Larrasoaña *et al.*, 2008; Fornaciari *et al.*, 2010; Agnini *et al.*, 2011).

Last occurrence of *Chiasmolithus grandis*. The presence of *C. grandis* in the Miralles-La Tossa composite section is rare and shows a discontinuous distribution. In the present study the last occurrence of this species has been recorded at sample MM012 at meter 610. Due to the scarcity of *C. grandis* at the section this bioevent could be considered an unreliable marker. However, the absence of both *C. grandis* and *C. oamaruensis* from sample MM013 to sample MM028 (meters 617 to 703.5) suggests that this part of the section corresponds to the upper part of Zone NP17. It is important to consider that the scarcity of *Chiasmolithus* is a generalized feature in the upper Eocene of the South Pyrenean foreland basin (Cascella and Dinarès-Turell, 2009) and Mediterranean area (Nocchi *et al.*,

1988; Luciani *et al.*, 2002) and thus, it is complex to accurately locate the base of Zone NP18 in these areas.

Last occurrence of *Sphenolithus obtusus*. Together with the last occurrence of *C. grandis*, the last occurrence of *S. obtusus* is used to mark the uppermost part of Zone NP17. In the Miralles-La Tossa composite section the last occurrence of *S. obtusus* has been recorded in sample MM014 (meter 624.5). This event confirms that from sample MM015 (meter 628.9) upward, the section corresponds, at least, to the uppermost part of Zone NP17.

The first occurrence of *Chiasmolithus oamaruensis* marks the base of Zone NP18. At the Miralles-La Tossa

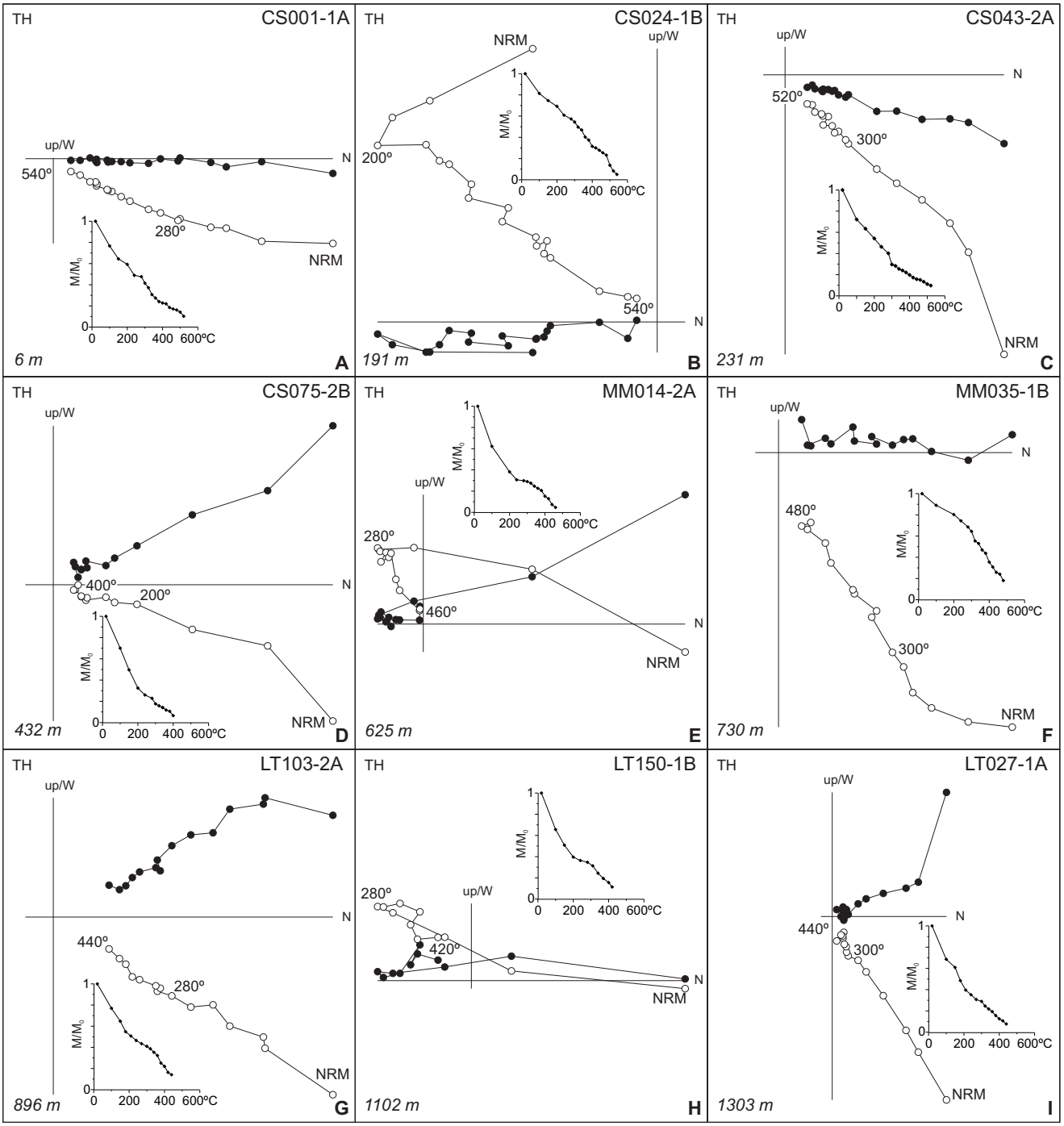

FIGURE 4 | Representative Zijderveld demagnetization diagrams from the Miralles-La Tossa composite section. All the projections are in tectonic corrected coordinates. The natural remanent magnetization decay plots (squared curve) are obtained after the normalization of the vector subtraction module. The stratigraphic position is shown in meters (lower left). A to F) Samples from the Miralles section. G to I) Samples from the La Tossa section.

composite section, this event has been recorded at sample LT100, located approximately 100 meters above the base of the Igualada Formation. Although *Chiasmolithus* specimens are scarce throughout the whole section, *C. oamaruensis* has been continuously recorded from sample LT100 (meter 875.3) upward.

The first occurrence of *Isthmolithus recurvus* marks the base of Zone NP19. At the Miralles-La Tossa composite section the first occurrence of *I. recurvus* has been recorded together with the first occurrence of *C. oamaruensis* at sample LT100 (metere 875.3) and as a result the record of Zone NP18 is missing. However, Zone NP18 could still be present in the upper 50 meters of the Collbàs Formation with scarce and poorly preserved calcareous nannofossils and/or in the non-outcropping 100m-thick interval of the base of the Igualada Formation.

Magnetostratigraphy

In the 1350m-thick composite section of Miralles-La Tossa a total of 224 paleomagnetic sites were collected. The mean sampling resolution obtained was of 6 meters in the Miralles section and of 4 meters in the La Tossa section, enough to allow a complete identification of this time period geomagnetic polarity reversals considering mean accumulation rates of 20-25cm/kyr reported along the eastern Ebro Basin (Burbank *et al.*, 1992a, b; Vergés and Burbank, 1996; Taberner *et al.*, 1999; Costa *et al.*, 2010). Sampling was focused on fine-grained fraction lithologies, mudstones and micritic limestones in the continental Pontils Group and gray marls, limestones and fine sandstones in the marine Igualada and Tossa formations and in the "Terminal Complex". Two oriented cores per site were taken with an electrical portable drill at most sites. Samples were oriented in situ using a magnetic compass coupled to a core-orienting fixture.

The paleomagnetic analysis consisted in stepwise thermal demagnetization of the natural remanent magnetization on at least one sample per site. Measurements of the natural remanent magnetization were performed using a 2G superconducting rock magnetometer at the Paleomagnetic Laboratory of the Universitat de Barcelona (CCiTUB-CSIC). Stepwise thermal demagnetization was conducted in a Schönstedt TSD-1 and a Magnetic Measurements MMTD-80 thermal demagnetizers at intervals ranging between 100°C and 20°C and up to a maximum temperature of 540°C.

Paleomagnetic components were determined from the visual inspection of Zijderveld diagrams (Fig. 4). In all the specimens, a viscous magnetization component which parallels the present day field and represents up to 70% of the initial natural remanent magnetization is unblocked at temperatures below 240°C to 280°C. Above this temperature, a characteristic remanent magnetization of either normal or reversed polarity can be identified. The characteristic remanent magnetization shows maximum unblocking temperatures above 300°C, which

A) Miralles-La Tossa (Stratigraphic)

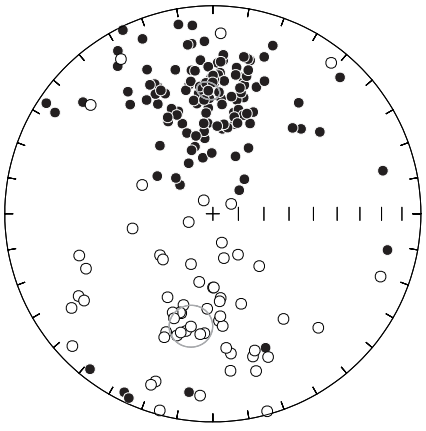

Polarity	N	Dec	Inc	k	α95
Normal	127	357.9	40.5	9.9	4.2
Reversed	61	191.0	-44.1	5.8	8.3

B) Miralles-La Tossa (Geographic)

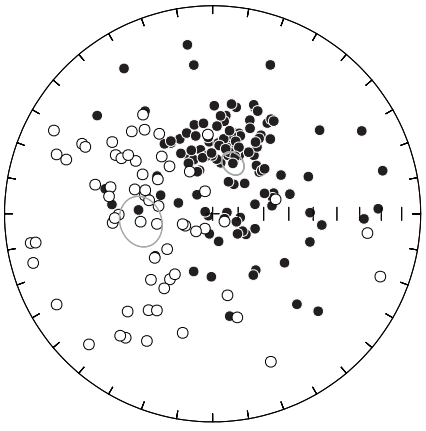

Polarity	N	Dec	Inc	k	α95
Normal	126	21.9	68.7	8.9	4.5
Reversed	62	263.8	-61.5	5.0	9.0

FIGURE 5 | Stereonet projections of the characteristic remanent magnetization of the Miralles-La Tossa composite section with calculated Fisherian statistics and mean. A) Stratigraphic and B) Geographic coordinates.

suggests that the characteristic remanent magnetization is carried by iron oxides such as magnetite and hematite. Characteristic remanent magnetization directions were calculated from the demagnetization diagrams by means of principal components analysis (Kirschvink, 1980). Reliable characteristic remanent magnetization directions were calculated for 186 paleomagnetic sites (Table III), which represent 83% of the total number of sampled levels. Normal and reversed characteristic remanent magnetization directions yield antipodal Fisherian means after the bedding correction (Fig. 5) and the obtained values conform to the paleomagnetic references for the Middle-Upper Eocene (Burbank *et al.*, 1992a; Taberner *et al.*, 1999).

Characteristic remanent magnetization directions were used to compute the latitude of the Virtual Geomagnetic Pole (VGP) in order to obtain a local magnetostratigraphy of the Miralles-La Tossa composite section (see Table III). Magnetozones were defined by at least two adjacent paleomagnetic sites with the same polarity. Single-site reversals were denoted as half-bar magnetozones in the local magnetostratigraphic section, but were not considered for magnetostratigraphic correlation purposes. After the exclusion of these unreliable short magnetic reversals, a total of 7 normal and 5 reversed polarity magnetozones have been recognized along the composite Miralles-La Tossa magnetostratigraphic section (Fig. 6).

CORRELATION OF THE MIRALLES-LA TOSSA MAGNETOSTRATIGRAPHIC SECTION TO THE GEOMAGNETIC POLARITY TIME SCALE

A correlation of the local magnetostratigraphic section of Miralles-La Tossa with the GPTS 2004 (Gradstein *et al.*, 2004) can be put forward on the basis of the available biostratigraphic constraints and the obtained polarity reversal pattern (Fig. 6). Biostratigraphic data discussed above clearly indicates that the marine units of the Miralles-La Tossa composite section span from Bartonian to Priabonian age. Taken biostratigraphy as a first-order coarse constraint, a good fit of the composite Miralles-La Tossa magnetostratigraphy with the GPTS (Gradstein *et al.*, 2004) is achieved by correlating the long reversed magnetozones R1 and R2 with the chrons C19r and C18r, and the long normal magnetozones N4, N5+N6, and N7 with chrons C18n, C17n, and C16n respectively (Fig. 6). Correlation of the top normal magnetozone N7 with chron C16n.2n is in agreement with the calcareous nannofossil data reporting a NP19-20 age, and best fits with the age of the marine-continental transition in the basin (Costa *et al.*, 2010). Following this solution, shorter chrons C17n.2n, C17n.1r, and C17n.2r must have been missed in the non outcropping gap corresponding to the lower part of the Igualada Formation. A short normal magnetozone at the transition from the continental Pontils Group to the Collbàs Formation (N3) is ignored in the proposed correlation. A delayed magnetization associated to this transition is suggested given the correspondence between polarity and sedimentary facies changes. Samples recording N3 correspond to lagoonal grey mudstones of the top Pontils Group, while samples recording R3 correspond to the transgressive coarse sediments of the basal Collbàs Formation.

The biomagnetostratigraphy-based chronology of the Miralles-La Tossa composite section allows establishing a reliable chronostratigraphy of the Middle-Upper Eocene marine record of the eastern Ebro Basin. The resulting absolute chronology, ranging from chron C20n to chron C16n (~43Ma to ~36Ma), challenges existing chronostratigraphic interpretations of the Pontils and Santa Maria groups (Fig. 2). While earlier studies attributed a Bartonian age to these units according to their fossil content (Serra-Kiel *et al.*, 2003b), the new magnetostratigraphy of Miralles-La Tossa sections demonstrates that the Igualada Formation embraces a large part of the Priabonian stage.

CALIBRATION OF THE BARTONIAN-PRIABONIAN SBZ AND NP BIOZONES

The Bartonian-Priabonian boundary as defined in the historical type section of Priabona (northern Italy) is loosely characterized because it corresponds to a transition from continental to marine facies (Luciani *et al.*, 2002; Gradstein *et al.*, 2004; Cascella and Dinarès-Turell, 2009; Agnini *et al.*, 2011). For that reason, biomagnetostratigraphic calibrations of the Priabonian stage have been to date based on the classic pelagic sections in Umbria, central Italy (Lowrie *et al.*, 1982; Monechi and Thierstein, 1985; Monechi, 1986), as well as on Ocean Drilling Program (ODP), Deep Sea Drilling Project (DSDP) and Integrated Ocean Drilling Program (IODP) sites (Poore *et al.*, 1982; Backman, 1987; Wei and Wise, 1989; Wei, 1991; Wei and Thiesrstein, 1991; Channell *et al.*, 2003). More recently, detailed biomagnetostratigraphic data from the ODP Site 1052 (northwestern Atlantic Ocean) and the Alano section (northern Iatly) have provided new insights on the calibration of the calcareous nannofossil zonation of the Middle-Late Eocene (Fornaciari *et al.*, 2010; Agnini *et al.*, 2011). Larger foraminiferal data are absent in these pelagic records, so that calibration of the SBZ scale has remained elusive to most recent calibration efforts of marine biostratigraphy. The new biomagnetostratigraphic data from the Miralles-La Tossa composite section allows an improved intercalibration between larger foraminifers and calcareous nannofossils as well as a new correlation with the GPTS.

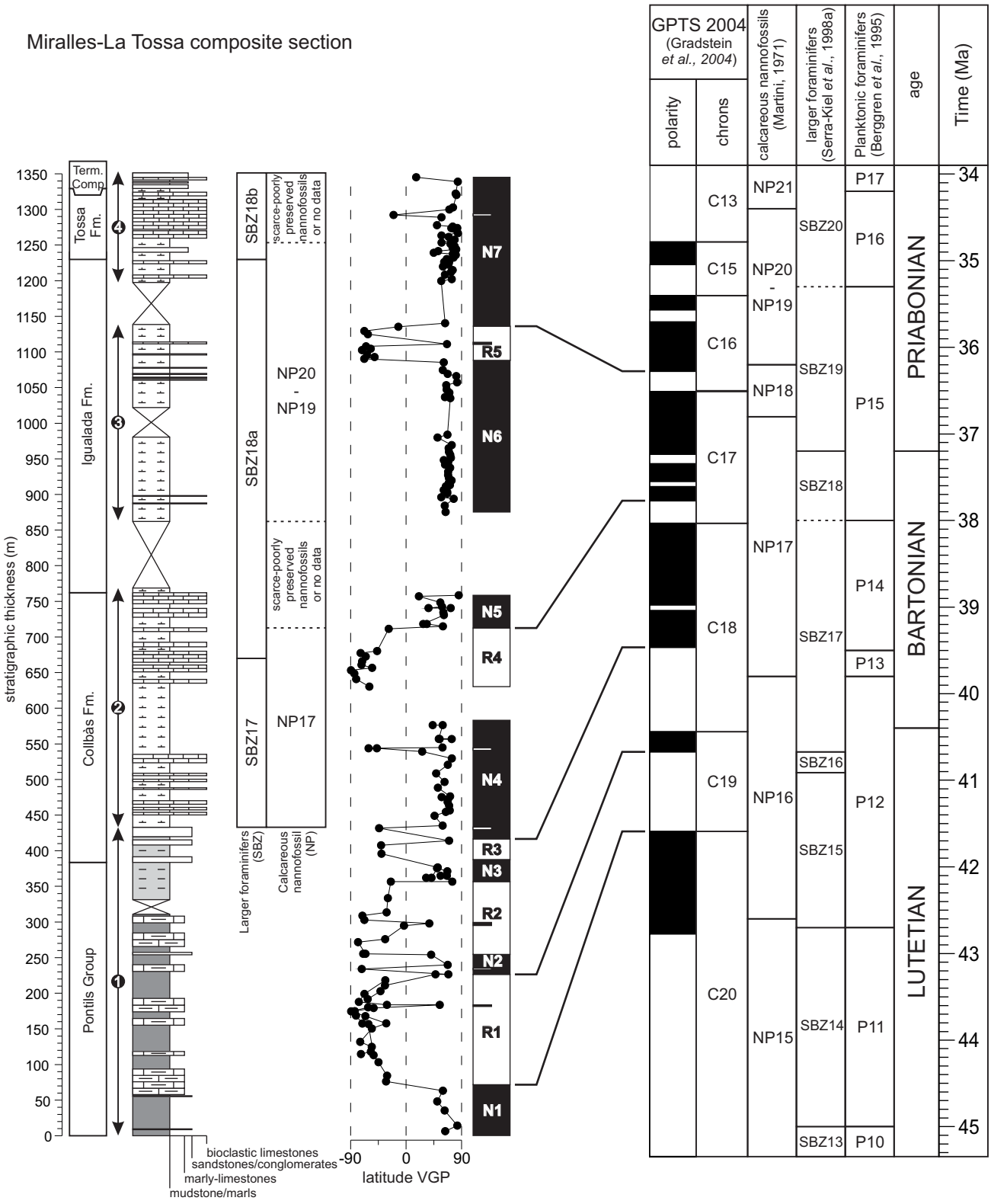

FIGURE 6 | Local magnetostratigraphic section of the Miralles-La Tossa and correlation to the GPTS (Gradstein *et al.*, 2004). Black dots show the Virtual Geomagnetic Pole (VPG) latitude. Stable magnetozones were defined by at least 2 adjacent paleomagnetic sites showing the same polarity. Half-bar zones denote single-site reversals. Calcareous nannofossil, larger foraminiferal and planktonic foraminiferal zonations come from Martini (1971), Serra-Kiel *et al.* (1998a) and Berggren *et al.* (1995), respectively. 1 to 4 correspond to subsections shown in Figure 1B.

Larger foraminifers

The current calibration of the larger foraminiferal biostratigraphy correlates zones SBZ17 and SBZ18 with the Bartonian (Serra-Kiel *et al.*, 1998a), the two zones being well represented in the fossil record of the Ebro Basin. According to Serra-Kiel *et al.* (1998a), Zone SBZ17 is defined by the biostratigraphic range of *Alveolina elongata*, *A. fragilis*, *A. fusiformis*, *Nummulites brongniarti*, *N. perforatus*, *N. hottingeri*, *N. puschi*, *N. biarritzensis*, *N. lyelli* and *Discocyclina pulcra baconica*. It is worth noting that during the thorough revision of the larger foraminiferal assemblages of the Miralles section, a transcription error in the work of Serra-Kiel *et al.* (2003a, b) was detected, which lead to an incorrect attribution of *Nummulites cyrenaicus*, *N. vicary* and *N. striatus* to Zone SBZ17. Zone SBZ18 is defined by the biostratigraphic range of *Nummulites biedai*, *N. cyrenaicus*, *N. vicaryi* and *N. boulangeri* (Serra-Kiel *et al.*, 1998a). The absence of these species in the Upper Eocene series of northern Italy has to date supported a correspondence of Zone SBZ18 with the Late Bartonian. Zone SBZ19, correlated with early Priabonian, is defined by the biostratigraphic range of *Nummulites fabianii*, *N. garnieri garnieri*, *N. cunialensis*, *Discocyclina pratti minor* and *Asterocyclina alticostata danubica*.

In the Geologic Time Scale 2004 (Gradstein *et al.*, 2004) no correlation of the Paleogene larger foraminiferal zonation with the GPTS is provided, therefore the only available calibration is the one proposed by Serra-Kiel *et al.* (1998a). These authors correlated zones SBZ17 and SBZ18 to the GPTS (Berggren *et al.*, 1995) according to the magnetostratigraphic data of Burbank *et al.* (1992a) in the equivalent marine units of the Vic area (Fig. 1A for location). The Vic magnetostratigraphy, however, was questioned by new biostratigraphic data from the same area (Cascella and Dinarès-Turell, 2009), and its correlation with the GPTS was re-interpreted in the light of new magnetostratigraphic constraints (Costa *et al.*, 2010). Therefore, a new calibration of the larger foraminiferal zonation is required.

The results of the present study (Fig. 3) provide further constraints for a revised calibration of zones SBZ17, SBZ18, and SBZ19 (Figs. 6; 7). It is shown that the entire Zone SBZ17 correlates with the Bartonian (Fig. 7). Zone SBZ18 spans from Late Bartonian to Early Priabonian, in contrast to its currently accepted Late Bartonian age. This new attribution is coherent with the presence of *N. stellatus* in the lowermost part of the Igualada Formation, a form which has been found in the Priabonian record of the Monte Cavro, Nago, Mossano (Papazzoni and Sirotti, 1995) and in the Marne di Possagno in northern Italy (Herb and Hekel, 1975). As a consequence, a division of Zone SBZ18 into two subzones (SBZ18a and SBZ18b) is here proposed. Subzone SBZ18a is characterized by the presence of *Nummulites vicaryi*, *Nummulites cyrenaicus*, *Nummulites biedai* and *Nummulites boulangeri*. Subzone SBZ18b is characterized by the presence of *Nummulites* aff. i*ncrassatus ramondiformis*, *Nummulites garnieri sturi*, *Nummulites chavannesi*, *Asterocyclina stellata*, *Pellatispira madaraszi*, *Heterostegina reticulate* and *Biplanispira absurda*, this Subzone being equivalent to the *Nummulites variolarius/incrassatus* Biozone of Papazzoni and Sirotti (1995).

The newly defined Subzone SBZ18b, spanning the Tossa Formation and the "Terminal Complex", correlates to the Mid-Priabonian (chron C16n). The fossil assemblage found in the "Terminal Complex" contains an association of *Malatyna vicensis*, *Orbitolites* sp. and *Rhabdorites malatyaensis*. Remarkably, this fossil assemblage is not known in the Priabonian type sections of northern Italy, probably because of paleoenvironmental issues.

Calcareous nannofossils

The Bartonian and Priabonian stages include the calcareous nannofossil zones NP17, NP18, and NP19-20 (Martini, 1971). The current calibration of the NP zones (Gradstein *et al.*, 2004) is largely based on the biomagnetostratigraphic correlations of Berggren *et al.* (1995). Following this scheme, the base of Zone NP17 (last occurrence of the *Chiasmolithus solitus*) correlates with the reversed chron C18r (Early Bartonian), the base of Zone NP18 (first occurrence of the *Chiasmolithus oamaurensis*) with chron C17n.1n (Early Priabonian), and the base of Zone NP19-20 (first occurrence of the *Isthmolithus recurvus*) with chron C16n.2n (Priabonian). Regarding the age of this last bioevent, debate has persisted in the literature. In Umbria, the first occurrence of *I. recurvus* was first correlated with chron C15 (Lowrie *et al.*, 1982; Monechi and Thierstein, 1985), but was later found to occur at an older age, within chron C16n.2n (Monechi, 1986), such discrepancy being attributed to the poor preservation or scarcity of *I. recurvus* in the Umbrian sections (Monechi, 1986). In oceanic sections of the Southern Ocean, the same event was found either in chron C15n in Site 522 (Poore *et al.*, 1982), or in chron C16n (in sites 522 and 523, Backman, 1987; sites 699A and 703A, Wei, 1991; Site 744A, Wei and Thiesrstein, 1991; Site 1090, Channell *et al.*, 2003), this diachrony being attributed to its cool water affinity (Backman, 1987; Wei and Wise, 1989; Wei, 1991).

In the eastern Ebro Basin, the new biomagneto-stratigraphy of the Miralles-La Tossa composite section indicates a correlation of first occurrence of *I. recurvus* with chron C17n.1n, an age which is considerably older than the records discussed above. Noteworthy, a correlation of this

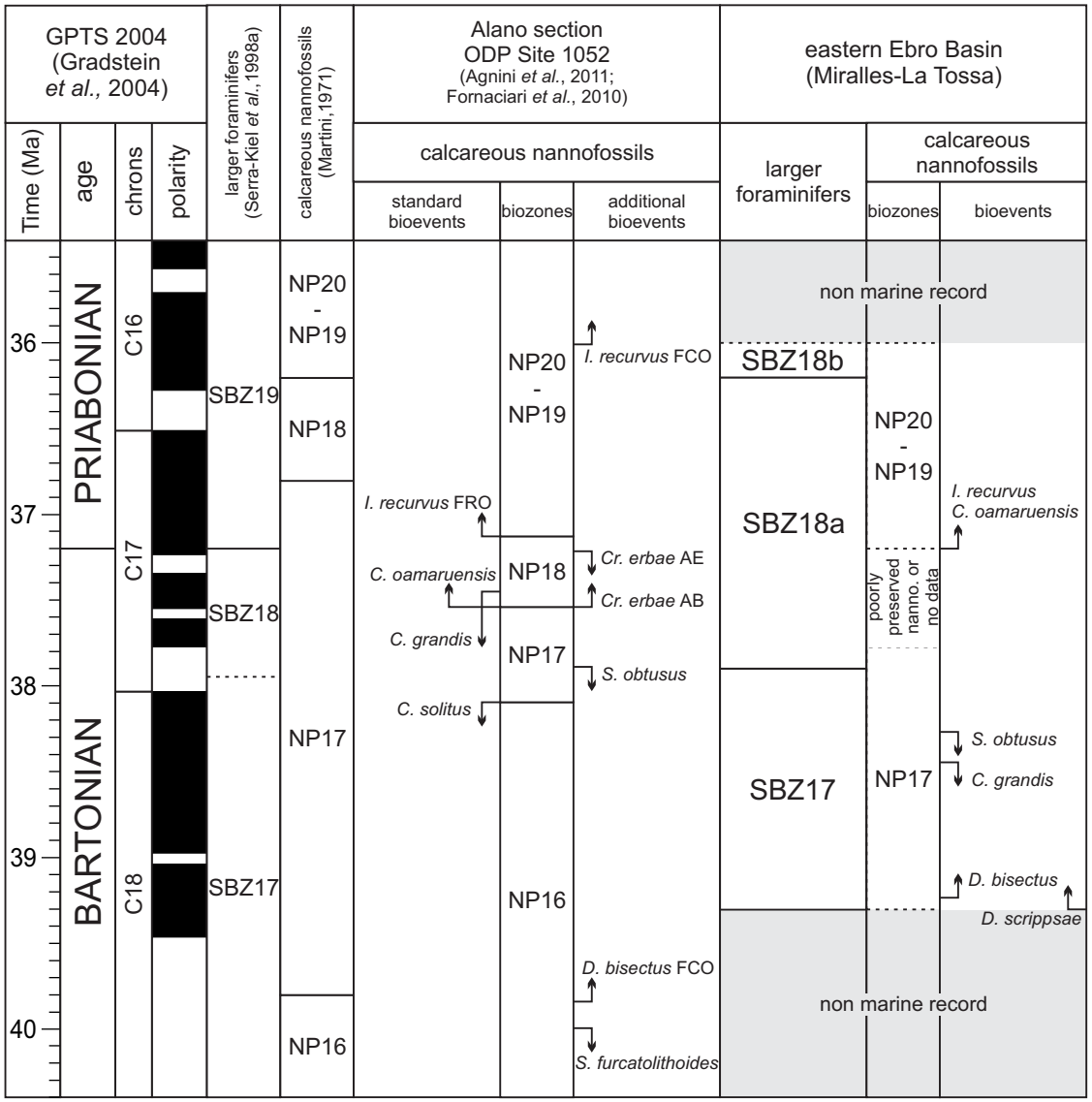

FIGURE 7 | New calibration of the Miralles-La Tossa larger foraminiferal and calcareous nanofossil zones to the GPTS (Gradstein *et al.*, 2004). Previous calibrations of these zonations (Martini, 1971; Serra-Kiel *et al.*, 1998a; Fornaciari *et al.*, 2010; Agnini *et al.*, 2011) are also shown to contrast. Discontinuous line indicates indeterminate zone boundary and grey colour indicates lack of marine record in the eastern Ebro Basin. FRO: First Rare Occurrence. FCO: First Common Occurrence. AB: Acme Beginning. AE: Acme End.

event with chron C17n was already reported from DSDP Site 516 (Wei and Wise, 1989), and Site 523 (Backman, 1987), both records regarded as unreliable: Site 516 was considered to yield poor-quality magnetostratigraphy (Channell *et al.*, 2003), while data from Site 523 were rejected arguing downhole contamination (Backman, 1987). Nevertheless, recent results from the ODP Site 1052 in the NW Atlantic Ocean (Fornaciari *et al.*, 2010) and the Alano section in the Possagno area, northern Italy, (Agnini *et al.*, 2011) firmly support a correlation of the First Rare Occurrence (FRO) of *I. recurvus* with chrons C17n.1r and C17n.1n (Fig. 7), in agreement with results from the Ebro Basin.

Extending the range of Zone NP19-20 down to chrons C17n.1n or C17n.1r, would lead to a complete overlap with the range of Zone NP18 (Fig. 7). This raises the question on whether the first occurrence of *I. recurvus* is a reliable long-distance chronostratigraphic marker, a question which is in agreement with the highlighted need to revise the present Middle-Late Eocene calcareous nannofossil biochronology pointed out by Fornaciari *et al.* (2010) and Agnini *et al.* (2011).

CONCLUSIONS

The combined biostratigraphic (calcareous nannofossils, larger foraminifers) and magnetostratigraphic study of the

Middle-Late Eocene marine units of the Igualada area (NE Spain) allows establishing a reliable chronostratigraphy of the Middle-Upper Eocene marine record of the eastern Ebro Basin. The resulting new chronology, that ranges from chron C20n to chron C16n (Bartonian-Priabonian), challenges existing chronostratigraphic attributions of the Igualada and Tossa formations (Santa Maria Group). As a result, a revised calibration of the Late Eocene larger foraminiferal and calcareous nannofossil biozonation is proposed. The traditional division of the Bartonian stage into two complete larger foraminiferal zones, SBZ17 and SBZ18, is challenged. Zone SBZ17 embraces most of the Bartonian, while Zone SBZ18 extends from late Bartonian to early Priabonian. In addition, a new Subzone (SBZ18b=N. *variolarius*/*incrassatus* Biozone), recognized in both the Ebro Basin and the Priabonian type sections of Italy, is proposed, while the Subzone SBZ18a is equivalent to the former Zone SBZ18 of Serra-Kiel *et al*. (1998a). Magnetostratigraphic calibration of calcareous nannofossils in the Ebro Basin reveals a mismatch with the current calibration of Zone NP19-20, suggesting that first occurrence of *I. recurvus* is a diachronic event, of low reliability for long-distance correlations. The calcareous nannofossil Zone NP19-20 correlates to the larger foraminiferal Zone SBZ18 (uppermost Bartonian-Early Priabonian).

ACKNOWLEDGMENTS

This paper has been developed in the framework of the Spanish MICINN projects: COFORSED CGL2010-17479/BTE, REMOSS 3D-4D CGL2007-66431-C02-02/BTE, INTERBIOSTRAT CGL2008-0809/BTE and CECME CGL-2011-23770. This research was supported by the research group of "Geodinàmica i Anàlisi de Conques" (2009 GGR 1198-Secretariat d'Universitats i Recerca del Departament d'Economia i Coneixement de la Generalitat de Catalunya) and the Research Institute GEOMODELS. We are grateful to Vanesa Pulido and Ruth Soto who assisted during fieldwork and laboratory analysis. The discussion, comments and suggestions of an anonymous reviewer, Jaume Dinarès-Turell and Simonetta Monechi have significantly improved this paper. E. Costa was funded by a PhD grant of the MICINN.

REFERENCES

Agnini, C., Fornaciari, E., Giusberti, L., Grandesso, P., Lanci, L., Luciani, V., Muttoni, G., Pälike, H., Rio, D., Spofforth, D.J.A., Stefani, C., 2011. Integrated biomagnetostratigraphy of the Alano section (NE Italy): A proposal for defining the middle-late Eocene boundary. Geological Society of America Bulletin, 123(5-6), 841-872. DOI: 10.1130/B30158.1

Agustí, J., Anadón, P., Arbiol, S., Cabrera, L., Colombo, F., Sáez, A., 1987. Biostratigraphical characteristics of the Oligocene sequences of North-Eastern Spain (Ebro and Campins Basins). Münchner Geowissenschaftliche Abhandlungen, 10, 35-42.

Anadón, P., 1978. El Paleógeno continental anterior a la transgresión Biarritziense (Eoceno medio) entre los ríos Gaià y Ripoll (provincia de Tarragona y Barcelona). Estudios Geológicos, 34, 341-440.

Anadón, P., Feist, M., 1981. Charophytes et Biostratigraphie du Paléogène Inférieur du bassin de l'Ebre oriental. Palaeontographica Abteilung B, 178, 143-168.

Anadón, P., Roca, E., 1996. Geological setting of the Tertiary basins of the Northeastern Spain. In: Friend, P.F., Dabrio, C.J. (eds.). Tertiary basins of Spain. The stratigraphic record of crustal kinematics. Cambridge, Cambridge University Press, World and Regional Geology, 6, 43-48.

Anadón, P., Cabrera, L., Guimerà, J., Santanach, P., 1985a. Paleogene strike-slip deformation and sedimentation along the southeastern margin of the Ebro Basin. In: Biddle, K.T., Christie-Blick, N. (eds.). Strike-slip tectonics and sedimentation. Society of Economic Paleontology and Mineralogy, 37 (Special Publications), 303-318.

Anadón, P., Marzo, M., Puigdefàbregas, C., 1985b. The Eocene fan-delta of Montserrat (Southeastern Ebro basin, Spain). In: Milà, M.D., Rosell, J. (eds.). 6th European Meeting Excursion Guidebook. Lleida, Institut d'Estudis Ilerdencs, 109-146.

Anadón, P., Vianey-Liaud, M., Cabrera, L., Hartenberger, J.L., 1987. Gisements à vertébrés du paléogène de la zone orientale du bassin de l'Ebre et leur apport à la stratigraphie. Paleontologia i Evolució, 21, 117-131.

Anadón, P., Cabrera, L., Colldeforns, B., Sáez, A., 1989. Los sistemas lacustres del Eoceno superior y Oligoceno del sector oriental de la Cuenca del Ebro. Acta Geologica Hispanica, 24(3-4), 205-230.

Anadón, P., Cabrera, L., Choi, S.J., Colombo, F., Feist, M., Sáez, A., 1992. Biozonación del Paleógeno continental de la zona oriental de la Cuenca del Ebro mediante carófitas; implicaciones en la biozonación general de carófitas de Europa occidental. Acta Geologica Hispanica, 27(1-2), 69-94.

Arbiol, S., Sáez, A., 1988. Sobre la edad oligocénica inferior del yacimiento de Santpedor (Cuenca del Ebro, provincia de Barcelona). Acta Geologica Hispanica, 23(1), 47-50.

Aubry, M.P., 1983. Biostratigraphie du Paléogène de l'Europe épicontinentale du Nord-Ouest, etude fondée sur les nannofossiles calcaires. Documents des Laboratoires de Géologie de Lyon, 89, 1-317.

Backman, J., 1987. Quantitative calcareous nannofossil biochronology of middle Eocene through early Oligocene sediment from DSDP Sites 522 and 523. Abhandlungen der Geologische Bundesanstalt, 39, 21-32.

Barberà, X., Cabrera, L., Marzo, M., Parés, J.M., Agustí, J., 2001. A complete terrestrial Oligocene magnetostratigraphy from the Ebro Basin, Spain. Earth and Planetary Science Letters, 187(1-2), 1-16. DOI: 10.1016/S0012-821(01)00270-9

Beaumont, C., Muñoz, J.A., Hamilton, J., Fullsack, J., 2000. Factors controlling the Alpine evolution of the Central

Pyrenees inferred from the comparison of observations and geodynamical models. Journal of Geophysical Research, 105(B4), 8121-8145. DOI: 10.1029/1999JB900390

Berggren, W.A., Kent, D.V., Swicher III, C.C., Aubry, M.P., 1995. A revised Cenozoic geochronology and chronostratigraphy. In: Berggren, W.A., Kent, D.V., Aubry, M.P., Hardenbol, P. (eds.). Geochonology, Time Scales and Global Stratigraphic Correlations. Tulsa, Society for Sedimentary Geology (SEMP), 54 (Special Publications), 129-212.

Bernaola, G., Orue-Etxebarria, X., Payros, A., Dinarès-Turell, J., Tosquella, J., Apellaniz, E., Caballero, F., 2006. Biomagnetostratigraphic analysis of the Gorrondatxe section (Basque Country, Western Pyrenees): Its significance for definition of the Ypresian/Lutetian boundary stratotype. Neues Jahrbuch für Geologie und Paläontologie Abhandlungen, 241, 67-109.

Bown, P.R., 1998. Calcareous Nannofossil Biostratigraphy. London, Chapman Hall Ltd. Kluwer Academic Publisher, 385pp.

Bralower, T.J., 2005. Data Report: Paleocene-early Oligocene calcareous nannofossil biostratigraphy, ODP Leg 198, Sites 1209, 1210, and 1211 (Shatsky Rise, Pacific Ocean). In: Bralower, T.J., Premoli-Silva, I., Malone, M.J. (eds.). Proceedings of the Ocean Drilling Project. Scientific Results, 198, 1-15. DOI: 10.2973/odp.proc.sr.198.104.2005

Burbank, D.W., Puigdefàbregas, C., Muñoz, J.A., 1992a. The chronology of the Eocene tectonic and stratigraphic development of the eastern Pyrenean foreland basin, northeast Spain. Gelogical Society of America Bulletin, 104(9), 1101-1120. DOI: 10.1130/0016-7606(1992)104<1101:TCOTET>2.3.CO;2

Burbank, D.W., Vergés, J., Muñoz, J.A., Bentham, P., 1992b. Coeval hindward- and forward-imbricating thrusting in the south-central Pyrenees, Spain: Timing and rates of shortening and deposition. Gelogical Society of America Bulletin, 104(1), 3-17. DOI: 10.1130/0016-7606(1992)104<0003:CHAFIT>2.3.CO;2

Cascella, A., Dinarès-Turell, J., 2009. Integrated calcareous nannofossil biostratigraphy and magnetostratigraphy from the uppermost marine Eocene deposits of the southeastern pyrenean foreland basin: evidences for marine Priabonian deposition. Geologica Acta, 7(1-2), 281-296. DOI: 10.1344/105.000000282

Caus, E., 1973. Bioestratigrafía y micropaleontología del Eoceno medio y superior del Prepirineo Catalán. Doctoral Thesis. Cerdanyola del Vallès, Universitat Autònoma de Barcelona, 186pp.

Caus, E., 1975. Bioestratigrafía del Eoceno medio y superior del Prepirineo Catalán (y la zona del tránsito entre esta unidad y la Cordillera Prelitoral Catalana). Revista Española de Micropaleontología, 7(2), 297-316.

Channell, J.E.T., Galeotti, S., Martin, E.E., Billups, K., Scher, H.D., Stoner, J.S., 2003. Eocene to Miocene magnetostratigraphy, biostratigraphy, and chemostratigraphy at ODP Site 1090 (sub-Antarctic South Atlantic). Gelogical Society of America Bulletin, 115(5), 607-623. DOI: 10.1130/0016-7606(2003)115<0607:ETMMBA>2.0.CO;2

Colom, G., 1971. Micropaleontología de las séries eocénicas de Santa Coloma de Queralt (Tarragona). Memorias de la Real Academia de Ciencias y Artes de Barcelona, 51(4), 73-135.

Costa, E., Garcés, M., López-Blanco, M., Beamud, E., Gómez-Paccard, M., Larrasoaña, J.C., 2010. Closing and continentalization of the South Pyrenean foreland Basin (NE Spain): Magnetochronological constraints. Basin Research, 22(6), 904-917. DOI: 10.1111/j.1365-2117.2009.00452.x

Cuevas, J.L., Cabrera, L., Marcuello, A., Arbués, P., Marzo, M., Bellmunt, F., 2010. Exhumated channel sandstone networks within fluvial fan deposits from the Oligo-Miocene Caspe Formation, South-east Ebro Basin (North-east Spain). Sedimentology, 57(1), 162-189. DOI: 10.1111/j.1365-3091.2009.01096.x

Ferrer, J., 1971a. El Paleoceno y Eoceno del borde suroriental de la Depresión del Ebro (Cataluña). Mémoires suisses de Paléontologie, 90, 1-70.

Ferrer, J., 1971b. Presencia de macroforaminíferos priabonienses en el Eoceno de Igualada. Acta Geologica Hispanica, 6(1), 4-7.

Fornaciari, E., Agnini, C., Catanzariti, R., Rio, D., Bolla, E.M., Valvasoni, E., 2010. Mid-Latitude calcareous nannofossil biostratigraphy and biochronology across the middle to late Eocene transition. Stratigraphy, 7(4), 229-264.

García-Castellanos, D., Vergés, J., Gaspar-Escribano, J., Cloetingh, S., 2003. Interplay between tectonics, climate, and fluvial transport during the Cenozoic evolution of the Ebro Basin (NE Iberia). Journal of Geophysical Research, 108(B7), 2347-2364. DOI: 10.1029/2002JB002073

Gaspar-Escribano, J., García-Castellanos, D., Roca, E., Cloetingh, S., 2004. Cenozoic vertical motions of the Catalan Coastal Ranges (NE Spain): the role of tectonics, isostasy, and surface transport. Tectonics, 23, 1-18. DOI: 10.1029/2003TC001511

Gradstein, F.M., Ogg, J.G., Smith, A.G., 2004. A Geologic Time Scale 2004. Cambridge, Cambridge University Press, 589pp.

Guimerà, J., 1984. Paleogene evolution of deformation in the northeastern Iberian Peninsula. Geological Magazine, 121(5), 413-420. DOI: 10.1017/S0016756800029940

Herb, R., Hekel, H., 1975. Nummulites aus dem Obereocaen von Possagno. Schweizerische Paläontologische Abhandlungen, 97, 113-211.

Hottinger, L., 1960. Recherches sur les Alvéolines du Paléocène et de l'Éocène. Mémoires suisses de Paléontologie, 75-76, 1-243.

Hottinger, L., Schaub, H., 1960. Zur Stufeneintelung des Paleocaens und des Eocaens. Einführung der Stufen Ilerdien und Biarritzien. Eclogae geologicae Helvetiae, 53, 453-480.

Hottinger, L., Romero, J., Caus, E., 2001. Architecture and revision of the Pellatispirines planispiral canaliferous foraminifera from the Late Eocene Tethys. Micropaleontology, 47(2, Supplement), 35-77.

Kapellos, C., Schaub, H., 1973. Zur Korrelation von Biozonierungen mit Grossforaminiferen und Nannoplankton im Paläogen der Pyrenäen. Eclogae geologicae Helvetiae, 66, 687-737.

Kirschvink, J.L., 1980. The least-squares line and plane and the analysis of paleomagnetic data. Geophysical Journal

of the Royal Astronomical Society, 62, 699-718. DOI: 10.1111/j.1365-246X.1980.tb02601.x

Langereis, C.G., Krijgsman, W., Muttoni, G., Menning, M., 2010. Magnetostratigraphy - concepts, definitions, and applications. Newsletter on Stratigraphy, 43(3), 207-233. DOI: 10.1127/0078-0421/2010/0043-0207

Larrasoaña, J.C., Gonzalvo, C., Molina, E., Monechi, S., Ortiz, S., Tori, F., Tosquella, J., 2008. Integrated magnetobiochronology of the Early/Middle Eocene transition at Agost (Spain): Implications for defining the Ypresian/Lutetian boundary stratotype. Lethaia, 41(4), 395-415. DOI: 10.1111/j.1502-3931.2008.00096.x

López-Blanco, M., 2002. Sedimentary response to thrusting and fold growing on the SE margin of the Ebro basin (Paleogene, NE Spain). Sedimentary Geology, 146(1-2), 133-154. DOI: 10.1016/S0037-0738(01)00170-1

López-Blanco, M., Marzo, M., Burbank, D.W., Vergés, J., Roca, E., Anadón, P., Piña, J., 2000. Tectonic and climatic controls on the development of foreland fan deltas: Montserrat and Sant Llorenç del Munt systems (Middle Eocene, Ebro Basin, NE Spain). Sedimentary Geology, 138(1-4), 17-39. DOI: 10.1016/S0037-0738(00)00142-1

Lowrie, W., Álvarez, W., Napoleone, G., Perch-Nielsen, K., Premoli-Silva, I., Toumarkine, M., 1982. Paleogene magnetic stratigraphy in Umbrian pelagic carbonate rocks: The Contessa sections, Gubbio. Gelogical Society of America Bulletin, 93(5), 414-432. DOI: 10.1130/0016-7606(1982)93<414:PMSIUP>2.0.CO;2

Luciani, V., Negri, A., Bassi, D., 2002. The Bartonian-Priabonian transition in the Mossano section (Colli Berici, north-eastern Italy): a tentative correlation between calcareous plankton and shallow-water benthic zonations. Geobios, 35 (Supplement 1), 140-149. DOI: 10.1016/S0016-6995(02)00055-4

Martini, E., 1971. Standard Tertiary and Quaternary calcareous nannofossil zonation. In: Farinaci, A. (ed.). Proceedings of the II Planktonic Conference, Roma 1970. Roma, Edizioni Tecnoscienza, 2, 739-785.

Meulenkamp, J.E., Sissingh, W., 2003. Tertiary palaeogeography and tectonostratigraphic evolution of the Northern and Southern Peri-Tethys platforms and the intermediate domains of the African-Eurasian convergent plate boundary zone. Palaeogeography, Palaeoclimatology, Palaeoecology, 196(1-2), 209-228. DOI: 10.1016/S0031-0182(03)00319-5

Monechi, S., 1986. Calcareous nannofossil events around the Eocene-Oligocene Boundary in the Umbrian Apennines (Italy). Palaeogeography, Palaeoclimatology, Palaeoecology, 57, 61-69. DOI: 10.1016/0031-0182(86)90006-4

Monechi, S., Thierstein, H.R., 1985. Late Cretaceous-Eocene nannofossil and magnetostratigraphic correlations near Gubbio, Italy. Marine Micropaleontology, 9(5), 419-440. DOI: 10.1016/0377-8398(85)90009-X

Muñoz, J.A., 1992. Evolution of a continental collision belt: ECORS-Pyrenees crustal balanced cross-section. In: McClay, K.R. (ed.). Thrust Tectonics. London, Chapman & Hall, 235-246.

Nocchi, M., Parisi, G., Monaco, P., Monechi, S., Madile, M., 1988. Eocene and Early Oligocene micropaleontology and paleoenvironments in SE Umbria, Italy. Palaeogeography, Palaeoclimatology, Palaeoecology, 67(3-4), 181-244. DOI: 10.1016/0031-0182(88)90154-X

Orue-Etxebarria, X., Bernaola, G., Baceta, J.I., Angori, E., Caballero, F., Monechi, S., Pujalte, V., Dinarès-Turell, J., Apellaniz, E., Payros, A., 2004. New constraints on the evolution of planktic foraminifera and calcareous nannofossils accross the Paleocene-Eocene boundary interval: The Zumaia section revisited. Neues Jahrbuch für Geologie und Paläontologie Abhandlungen, 234, 223-259.

Papazzoni, C.A., Sirotti, A., 1995. Nummulite biostratigraphy at the Middle/Upper Eocene boundary in the northern Mediterranean area. Rivista Italiana di Paleontologia e Stratigrafia, 101(1), 63-80.

Pérez-Rivarés, F.J., Garcés, M., Arenas, C., Pardo, G., 2002. Magnetocronología de la sucesión miocena de la Sierra de Alcubierre (sector central de la Cuenca del Ebro). Revista de la Sociedad Geológica de España, 15(3-4), 211-225.

Plaziat, J.C., 1981. Late Cretaceous to Late Eocene paleogeographic evolution of southwest Europe. Palaeogeography, Palaeoclimatology, Palaeoecology, 36(3-4), 263-320. DOI: 10.1016/0031-0182(81)90110-3

Poore, R.Z., Tauxe, L., Percival, S.F.Jr., LaBrecque, J.L., 1982. Late Eocene-Oligocene magnetostratigraphy and biostratigraphy at South Atlantic DSDP Site 522. Geology, 10(10), 508-511. DOI: 10.1130/0091-7613(1982)10<508:LEMABA>2.0.CO;2

Pueyo, J.J., 1974. Estudio petrológico y geoquímico de los yacimientos potásicos de Cardona, Súria, Sallent y Balsareny (Barcelona, España). Doctoral Thesis. Barcelona, Universitat de Barcelona, 351pp.

Reguant, S., 1967. El Eoceno Marino de Vic (Barcelona). Memorias del Instituto Geológico y Minero de España. Madrid, Instituto Geológico y Minero de España, Tomo LXVIII, 350pp.

Riba, O., Reguant, S., Villena, J., 1983. Ensayo de síntesis estratigráfica y evolutiva de la cuenca terciaria del Ebro. In: Comba, J.A. (ed.). Geología de España. Libro Jubilar J.M. Ríos. Madrid, Instituto Geológico y Minero de España, Tomo II, 131-159.

Roca, E., Sans, M., Cabrera, L., Marzo, M., 1999. Oligocene to Middle Miocene evolution of the central Catalan margin (northwestern Mediterranean). Tectonophysics, 315(1-4), 209-233. DOI: 10.1016/S0040-1951(99)00289-9

Romero, J., 1996. Estudio de los foraminíferos bentónicos del límite Eoceno Medio-Eoceno Superior de la Cuenca de Igualada. Master Degree Thesis. Barcelona, Universitat de Barcelona, 184pp.

Romero, J., 2001. Los macroforaminíferos del Eoceno Medio del borde suroriental de la Cuenca Paleógena Surpirenaica. Doctoral Thesis. Cerdanyola del Vallès, Univeristat Autònoma de Barcelona, 349pp.

Romero, J., Hottinger, L., Caus, E., 1999. Early appearence of larger foraminifera supposedly characteristic for Late

Eocene in the Igualada Basin, NE Spain. Revista Española de Paleontología, 14(1), 79-92.

Rosell, J., Juliá, R., Ferrer, J., 1966. Nota sobre la estratigrafía de unos niveles con Carófitas existentes en el tramo rojo de la base del Eoceno al S de los Catalánides (Provincia de Barcelona). Acta Geologica Hispanica, 1(5), 17-20.

Roveda, V., 1961. Contributo allo studio di alcuni macroforaminiferi di Priabona. Rivista Italiana di Paleontologia, 67(2), 153-225.

Ruiz de Gaona, M., 1952. Resultado del estudio de los foraminíferos del Nummulítico de Montserrat y regiones limítrofes. Estudios Geológicos, 15, 21-28.

Ruiz de Gaona, M., Colom, G., 1950. Estudios sobre las sinencias de los foraminíferos eocénicos de la vertiente meridional del Pirineo (Cataluña-Vizcaya). Estudios Geológicos, 12, 293-434.

Sáez, A., 1987. Estratigrafía y sedimentología de las formaciones lacustres del tránsito Eoceno-Oligoceno del noreste de la cuenca del Ebro. Doctoral Thesis. Barcelona, Universitat de Barcelona, 353pp.

Schaub, H., 1981. Nummulites et Assilines de la Tethys Paléogène. Taxonomie, phylogénèse et biostratigraphie. Mémoires Suisses de Paléontologie, 104-106, 1-236.

Serra-Kiel, J., 1984. Estudi dels *Nummulites* del grup *N. perforatus* (Montfort). Treballs de la Institució Catalana d'Història Natural, 11, 1-244.

Serra-Kiel, J., Hottinger, L., Caus, E., Drobne, K., Ferràndez-Cañadell, C., Jauhri, A.K., Less, G., Pavlovec, R., Pignatti, J., Samsó, J.M., Schaub, H., Sirel, E., Strougo, A., Tambareau, Y., Tosquella, J., Zakrevskaya, E., 1998a. Larger Foraminiferal Biostratigraphy of the Tethyan Paleocene and Eocene. Bulletin de la Société géologique de France, 169(2), 281-299.

Serra-Kiel, J., Hottinger, L., Drobne, K., Ferràndez-Cañadell, C., Jauhri, A.K., Less, G., Pignatti, J., Samsó, J.M., Schaub, H., Sirel, E., Tambareau, Y., Tosquella, J., Zakrevskaya, E., 1998b. Larger benthic foraminifera. In: Thierry, J., Farley, M.B., Jacquin, Th., Graciansky, P.C., Vail, P.R. (eds.). Mesozoic-Cenozoic sequence stratigraphy of European basins. Society of Economic Paleontologist and Mineralogist, 60(3, Special Publications), 767pp.

Serra-Kiel, J., Mató, E., Saula, E., Travé, A., Ferràndez-Cañadell, C., Busquets, P., Samsó, J.M., Tosquella, J., Barnolas., A., Àlvarez-Pérez, G., Franquès, J., Romero, J., 2003a. An inventory of the marine and transitional Middle/Upper Eocene deposits of the Southeastern Pyrenean Foreland Basin (NE Spain). Geologica Acta, 1(2), 201-229. DOI: 10.1344/105.000001610

Serra-Kiel, J., Travé, A., Mató, E., Saula, E., Ferràndez-Cañadell, C., Busquets, P., Tosquella, J., Vergés, J., 2003b. Marine and Transitional Middle/Upper Eocene Units of the Southeastern Pyrenean Foreland Basin (NE Spain). Geologica Acta, 1(2), 177-200. DOI: 10.1344/105.000001609

Taberner, C., Dinarès-Turell, J., Giménez, J., Docherty, C., 1999. Basin infill architecture and evolution from magnetostratigraphic cross-basin correlations in the southeastern Pyrenean foreland basin. Geological Society of America Bulletin, 111(8), 1155-1174. DOI: 10.1130/0016-7606(1999)111<1155:BIAAEF>2.3.CO;2

Tosquella, J., 1995. Els Nummulitinae del Paleocè-Eocè inferior de la conca sudpirinenca. Doctoral Thesis. Barcelona, Universitat de Barcelona, 581pp.

Travé, A., 1992. Sedimentologia, petrologia i geoquímica (elements traça i isòtops) dels estromatòlits de la Conca Eocena Sudpirinenca. Doctoral Thesis. Barcelona, Universitat de Barcelona, 396pp.

Travé, A., Serra-Kiel, J., Zamarreño, I., 1996. Paleoecological interpretation of transitional enviroments in Eocene carbonates (NE Spain). Palaios, 11(2), 141-160.

Urgelés, R., Camerlenghi, A., Garcia-Castellanos, D., De Mol, B., Garcés, M., Vergés, J., Haslam, I., Hardman, M., 2011. New constraints on the Messinian sealevel drawdown from 3D seismic data of the Ebro Margin, western Mediterranean. Basin Research, 23(2), 123-145. DOI: 10.1111/j.1365-2117.2010.00477.x

Vergés, J., Burbank, D.W., 1996. Eocene-Oligocene thrusting and basin configuration in the eastern and central Pyrenees (Spain). In: Friend, P.F., Dabrio, C.J. (eds.). Tertiary basins of Spain. The stratigraphic record of crustal kinematics. Cambridge, Cambridge University Press, World and Regional Geology, 6, 120-133.

Vergés, J., Fernàndez, M., Martínez, A., 2002. The Pyrenean orogen: pre-, syn-, and post-collisional evolution. In: Rousenbaum, G., Lister, G.S. (eds.). Reconstruction of the Evolution of the Alpine-Himalayan Orogen. Journal of the Virtual Explorer, 8, 55-74. DOI: 10.3809/jvirtex.2002.00058

Virgili, C., 2007. Lyell and the Spanish Geology. Geologica Acta, 5(1), 119-126. DOI: 10.1344/105.000000314

Wei, W., 1991. Middle Eocene-lower Miocene calcareous nannofossil magnetobiochronology of ODP Holes 699A and 703A in the subantartic South Atlantic. Marine Micropaleontology, 18(1-2), 143-165. DOI: 10.1016/0377-8398(91)90010-4

Wei, W., Thierstein, H.R., 1991. Upper Cretaceous and Cenozoic calcareous nannofossils of the Kerguelen Plateau (Southern Indian Ocean) and Prydz Bay (East Antarctica). Proceedings of the Ocean Drilling Program, Scientific Results, 119, 467-493. DOI: 10.2973/odp.proc.sr.119.165.1991

Wei, W., Wise, S.W., 1989. Paleogene Calcareous Nannofossil Magnetobiochronology: Results from South Atlantic DSDP Site 516. Marine Micropaleontology, 14(1-3), 119-152.

Zoetemeijer, R., Desegaulx, P., Cloetingh, S., Roure, F., Moretti, I., 1990. Lithospheric dynamics and tectonic-stratigraphic evolution of the Ebro Basin. Journal of Geophysical Research, 95(B3), 2701-2711. DOI: 10.1029/JB095iB03p02701

Manuscript received December 2010;
revision accepted July 2011;
published Online April 2012.

ELECTRONIC APPENDIX

LARGER FORAMINIFERS

Recorded Assemblages

During the preparation of the present study, several mistakes in the larger foraminiferal biostratigraphic contents of previous studies performed in the Igualada area (Serra-Kiel *et al*., 2003a, b) were revealed. Specifically, *Nummulites cyrenaicus*, *N. vicary* and *N. striatus* were incorrectly attributed to zone SBZ17 in Serra-Kiel *et al*. (2003b) because of a transcription error in the Santa Maria de Miralles section of Serra-Kiel *et al*. (2003a). As an example, sample BM010 of the present study corresponds to a monospecific bank of *N. perforatus* in accordance with Serra-Kiel and Reguant (1984) and Teixell and Serra-Kiel (1988). It is the very same level as point 2 of Serra-Kiel *et al*. (2003a), but in that paper the fossil content is erroneously listed as containing *N. cyrenaicus*, *N. vicaryi*, *N. ptukhiani*, *N. praegarnieri*, *N. variolarius* and *Assilina schwageri*. Moreover, biostratigraphical contents of point 1 and point 5 in figure 28 of Serra-Kiel *et al*. (2003a) occurs to be the same. For that reason, the data of the Santa Maria de Miralles section of Serra-Kiel *et al*. (2003a) has not been taken into account in the present study.

Bellow, a complete and detailed list of the biostratigraphical content for all the samples and their correspondence to type localities along the Miralles-La Tossa composite section and Puig Aguilera (Fig. I.1 for location) is provided.

Sample BM005 (meter 446), at the bottom of the Collbàs Formation, contains *Nummulites biarritzensis* DE LA D'ARCHIAC and HAIME 1853, *Nummulites beaumonti* D'ARCHIAC and HAIME 1853 and *Nummulites praegarnieri* SCHAUB 1981 (Fig. I.7, 1-2).

Sample BM010 (meter 470.2) corresponds to a stratigraphic level characterized as a monospecific bank of *Nummulites perforatus* DE MONTFORT 1808 (Figs. I.3, 4-7; I.10, 6-10) by Serra-Kiel and Reguant (1984) and Teixell and Serra-Kiel (1988). The top of this level also contains *Alveolina fragilis* HOTTINGER 1960.

Sample MM004 (meter 509.8) corresponds to the type locality of *Nummulites hottingeri* SCHAUB 1981 (Figs. I.3, 1; I.10, 5) associated with *N. biarritzensis* (Figs. I.2, 5-7; I.9, 9-12) and *N. beaumonti*.

Sample MM007 (meter 524.5) contains *N. biarritzensis*, *N. beaumonti* and *Assilina schwageri* SILVESTRI 1928.

Sample MM008 (meter 536.0) corresponds to the type locality of *N. praegarnieri* associated with *N. beaumonti* (Figs. I.2, 1-2; I.9, 1-6), *A. schwageri* (Figs. I.11, 11-12) and *Operculina roselli* HOTTINGER 1977.

Sample MM022 (meter 660.0) contains *N. hottingeri* (Figs. I.3, 2-3; I.10, 1 to 4), *N. biarritzensis* (Figs. I.2, 8; I.9, 13) and *N. beaumonti* (Figs. I.2, 3-4; I.9, 7-8).

Sample MM024 (meter 680.0) contains *Nummulites vicaryi* SCHAUB 1981, *A. schwageri* and *O. roselli* (Fig. I.11, 10).

Sample MM028-29 (meter ~707.0) contains *Nummulites striatus* BRUGUIÈRE 1792, *N. vicaryi* (Figs. I.4, 1-5; I.11, 1-6) and *A. schwageri*.

Sample MM050, at the top of the Collbàs Formation, contains *N. striatus* (Figs. I.5, 2; I.12, 1 and 3).

Sample LT000 (meter ~825.0), at the lower part of the Igualada Formation, contains *Nummulites stellatus* ROVEDA 1961 (Figs. I.4, 6 and 7; I.11, 7 and 8) and *Nummulites orbignyi* GALEOTTI 1837.

Sample LT104 (meter 901.4) contains *N. striatus* (Figs. I.5, 1 and 3; I.12, 2, 4 and 5), *N. stellatus* (Fig. I.4, 8 and 9) and *N. orbignyi*.

Sample LT157 (meter 1135.2) contains *N. orbignyi* (Figs. I.4, 10; I.11, 9).

Sample LT163 (meter 1208.3) contains D*iscocyclina augustae augustae* WEIJDEN 1840, *Discocyclina radians radians* D'ARCHIAC 1850 and *Asterocyclina stellaris* BRÜNNER 1848 in RÜTIMEYER 1850.

Sample LT005 (meter 1237.5), from the La Tossa Formation, contains *Assilina schwageri*, *O. roselli*, *Asterocyclina stellata* D'ARCHIAC 1846, *Nummulites chavannesi* DE LA HARPE 1878 (Figs. I.6, 1-9; I.13, 6-11), *Nummulites garnieri sturi* VANOVA 1972 (Figs. I.7, 14-18; I.13, 1-5), *Nummulites "ptukhiani"* sensu Papazzoni (1998), and *Nummulites* aff. *incrassatus ramondiformis* DE LA HARPE 1883 (Figs. I.8, 1-5; I.13, 12-26).

In the nearest Puig Aguilera area (Fig. I.1), the Tossa Formation contains *Nummulites* aff. *incrassatus ramondiformis*, *N. chavanesi*, *N. garnieri sturi*, *N. "ptukhiani"*, *Operculina roselli*, *Assilina schwageri*,

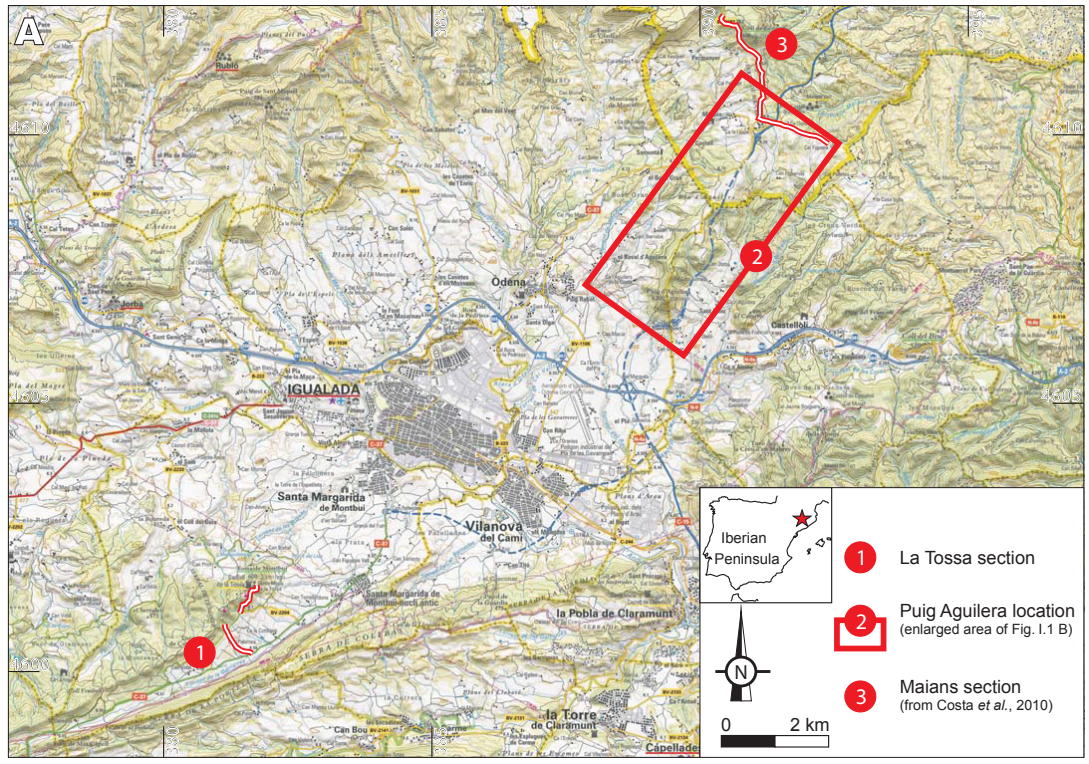

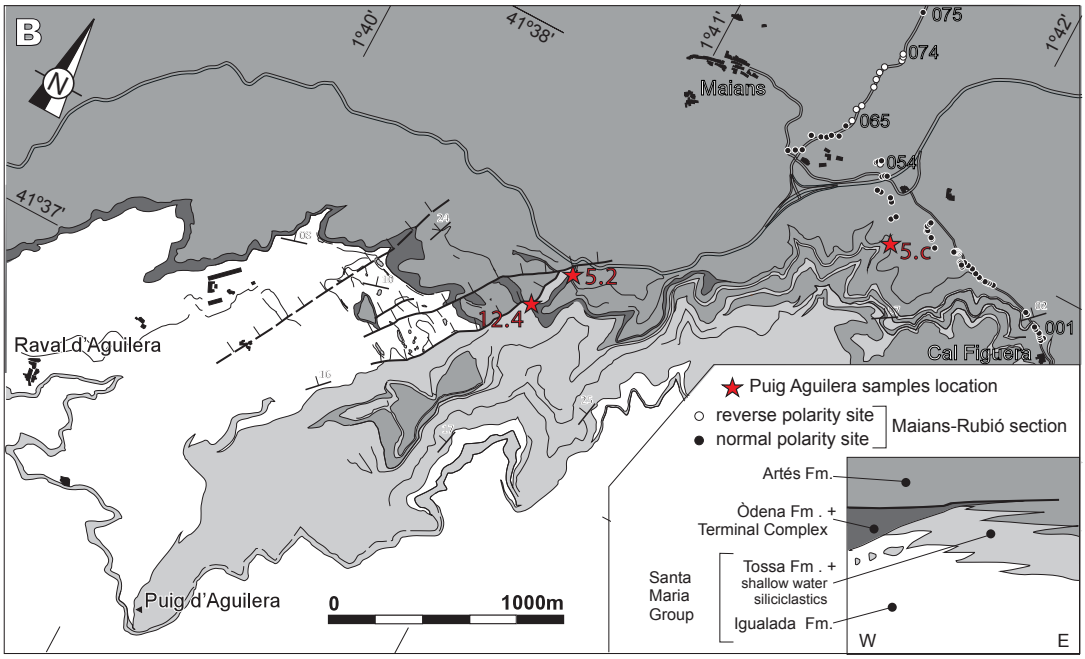

C

Sample	Unit	Facies	UTM coordinates (ED50 / zone 31N) x	y	z
5.2	Terminal Complex	marine limestone / larger foraminifers	390318.1214	4609173.713	556
5.c	Terminal Complex	marine limestone / larger foraminifers	391515.1564	4609982.287	544
12.4	Terminal Complex	marine limestone / larger foraminifers	390220.9346	4608940.702	565

FIGURE I.1 Larger foraminifers samples location of the "Terminal Complex" in Puig Aguilera (Igualada area, eastern Ebro Basin). A) Geographic location of the Puig Aguilera and La Tossa section. B) Detailed geological map with the location of the larger foraminifers samples of the "Terminal Complex" of Puig Aguilera. A sketched lithostratigraphic panel displaying lateral and vertical relationship between the marine and continental facies in the eastern part of the Igualada area is also shown. The black or white dots correspond to normal or reversed paleomagnetic sites of the lowermost Maians-Rubió section (Costa *et al.*, 2010). C) UTM coordinates (ED50/zone 31N).

Heterostegina reticulata RÜTIMEYER 1850, *Discocyclina pratti* MICHELIN 1846, *D. radians radians*, *D. augustae olianae*, *Asterocyclina stellaris*, *A. stellata*, *Orbitoclypeus varians* KAUFMANN 1867, *Pellatispira madaraszi* HANTKEN 1875 and *Biplanispira absurda* UMGROVE 1938. A detailed stratigraphical distribution of all this forms (white dots in Fig. 3) at the Puig Aguilera section is presented in Serra-Kiel *et al.* (2003a). Finally, the study of the samples collected in the "Terminal Complex" of Puig Aguilera (Fig. I.1) has revealed the presence of *Malatyna vicensis* SIREL and AÇAR 1998, *Rhabdorites malatyaensis* SIREL 1976 and *Orbitolites* sp. (marked as grey dots in Fig. 3).

Systematic Remarks

An accurate description of *Nummulites chavannesi*, *Nummulites garnieri sturi* and *Nummulites* aff. *incrassatus ramondiformis* from the Miralles-La Tossa composite section is provided in order to help comparison with specimens of these forms described in Priabona and Mossagno areas in Italy, Upper Hron depression in Slovakia, and the western Alps in France (Roveda, 1961; Vanova, 1972; Herb and Hekel, 1973, 1975; Schaub, 1981; Papazzoni and Sirotti, 1995) (Figs. I.6; I.7; I.8).

Family: Nummulitidae DE BLAINVILLE, 1825
GENUS Nummulites LAMARK, 1801
Nummulites chavannesi DE LA HARPE 1878
Figures I.6, 1 to 9; I.13, 6 to 11

1961 Nummulites chavanessi DE LA HARPE, Roveda (1961), pp- 177-181, pl. 14, figs. 1-8.
1975 Nummulites chavanessi DE LA HARPE, Herb and Hekel (1975), pp-123-125, pl. 2, figs. 1-3; Text-fig. 14-21.
2002 Nummulites chavannesi DE LA HARPE, Luciani et al. (2002), fig. 4 (2-4) and fig. 6.

Material. 16 specimens in the sample LT005 (Miralles-La Tossa composite section).

Description. Test lenticular flattened in the external zone with sharp periphery. The external view permits to observe the last marginal cord. The chambers are subromboidal in outline, with an aspect ratio (height/length)>1, and with arcuate ceiling. Septa are gently inclined to perpendicular and recurved towards periphery. The ornamentation consists of a coarse granule at the polar zone with radial filaments sinuous with S-form in the external zone. The spiral is thin and the growth is slightly irregular. The diameter of the proloculus in A-Forms is between 0.140-0.230mm (mean 0.180mm). Table I.1 sumarizes the biometric data of this species in the Miralles-La Tossa composite section.

Remarks. With the exception of the specimen illustrated in Figure I.6, 13, the A- and B-Forms from the Priabona area (Roveda, 1961; reproduced in Fig. I.6, 10-13) have greater test than the specimens from the Tossa Formation (Figs. I.6, 1-9; I.13, 6-11). The A-Form from the Marne di Possagno (Herb and Hekel, 1975) reproduced in Figures I.6, 14-17, in the lowermost part of the Cunial-Santa Giustina-Col dell'Asse section, have test and proloculus smaller in diameter than the specimens from the Tossa Formation. On the other hand, the A- and B-Forms from the Calcare di Santa Giustina and Marne siltose (Herb and Hekel, 1975), at the middle and lowermost part of the Cunial-Santa Giustina-Col dell'Asse section (Fig. I.6, 18 -20), are of greater size and shown a spiral growth less tight than our material. Whether this variability is intraspecific or corresponds to different chronospecies within the same lineage is not determined. Unfortunately, we have not enough material to clarify this question, and we prefer to use the specific terminology as evolutive species.

Nummulites chavannesi differs from the *Nummulites* aff. *incrassatus ramondiformis* for having sinuous filaments, thinner marginal cord, higher chambers and curved and more irregular spiral growth. *Nummulites chavannesi* differs from *Nummulites garnieri garnieri* for the type of the ornamentation, pattern of the spiral growth, and the size and outline of the chambers.

Nummulites garnier sturi BOUSSAC 1911
Figures I.7, 14 to 18; I.13, 1 to 5

1972 Nummulites garnieri sturi n. sp. Vanova (1972), pp-56-59, pl. 6, figs. 5-9; pl. 7 figs. 1-9; pl. 8 figs. 1-8
1995 Nummulites garnieri garnieri DE LA HARPE, Papazzoni and Sirotti (1995), pl. 2, figs. 6-7

Material. 12 specimens in the sample LT005 (Miralles-La Tossa composite section).

Description. Test lenticular with rounded periphery. The ornamentation consists of granules and filaments. The filaments are sinuously curved in S-form in the periphery. The granules are distributed at the polar zone and over the filaments towards the periphery. The chambers have an aspect ratio>1, with rhomboidal outline and arcuate ceiling. The septa are straight, slightly inclined towards the periphery. The spiral growth is regular, but slightly irregular in B-Form. The diameter of the proloculus is between 0.090-0.140mm (mean 0.125mm). Table I.2 sumarizes the biometric data of this species in the Miralles-La Tossa composite section.

Remarks. We consider the specimens of the sample LT005 as *Nummulites garnieri sturi* (Figs. I.7, 14-18; I.13, 1-5). They have a test size and diameter of the proloculus (0.090-0.140mm) greater than *Nummulites praegarnieri* (0.100-0.120mm) (Fig. I.7, 1-4), and similar to the forms described by Vanova (1972) (Fig. I.7, 5 to 7). *Nummulites*

TABLE I.1 Biometric data of 16 specimens of A- and B-Forms of Nummulites chavannesi from sample LT005

Dimensions of the B-Form in mm (4 specimens measured)						
	Max	Min	Mean			
Diameter	4.74	4.28	4.50			
Equatorial section (mean values)						
Whorld	1	2	3	4	5	6
Radius	0.30	0.50	0.78	1.15	1.60	2.00
Chambers	11	14	21	25	28	29
Dimensions of the A-Form in mm (12 specimens measured)						
	Max	Min	Mean			
Diameter	3.00	2.60	2.90			
Equatorial section (mean values)						
Whorld	1	2	3	4	5	
Radius	0.30	0.50	0.70	1.15	1.35	
Chambers	7	14	17	22	26	

TABLE I.2 Biometric data of 12 specimens of A- and B-Forms of Nummulites garnieri sturi from sample LT005

Dimensions of the B-Form in mm (4 specimens measured)						
	Max	Min	Mean			
Diameter	4.90	3.64	4.35			
Equatorial section (mean values)						
Whorld	1	2	3	4	5	6
Radius	0.25	0.47	0.75	1.00	1.50	2.00
Chambers	10	15-16	19-20	24	29-30	35
Dimensions of the A-Form in mm (8 specimens measured)						
	Max	Min	Mean			
Diameter	2.70	2.20	2.50			
Equatorial section (mean values)						
Whorld	1	2	3	4	5	6
Radius	0.25	0.45	0.60	0.90	1.25	1.65
Chambers	11-12	17	22-23	25	28-30	30

garnieri sturi from the Tossa Formation have smaller test and proloculus diameter than *Nummulites garnieri* (0.150-0.200mm) described by Schaub (1981) (Figs. I.7, 19 and 20) and *Nummulites garnieri garnieri* described by Herb and Hekel (1973) (Fig. I.7, 21 and 22). We consider *Nummulites garnieri garnieri* (Fig. I.7, 8-13) illustrated by Herb and Hekel (1975) as a synonym of *Nummulites garnieri sturi* (Fig. I.7, 5-7 and 14-18) because it yields the same test size and proloculus diameter. Finally, the succession of chronospecies of the *Nummulites garnieri* lineage, from Bartonian to uppermost Priabonian, consists of *Nummulites praegarnieri* SCHAUB 1981, *Nummulites garnieri sturi* VANOVA 1972, *Nummulites garnieri* sensu Schaub (1981) and *Nummulites garnieri inaequalis* HERB and HEKEL 1975 (Fig. A1.7, 23-26).

Nummulites aff. *incrassatus ramondiformis* DE LA HARPE 1883
Figures I.8, 1-5; I.13, 12-26

Material. 14 specimens in the sample LT005 (Miralles-La Tossa composite section).

Description. Test inflated lenticular with rounded periphery. The chambers are subromboidal in outline, isometric or with an aspect ratio slightly larger than 1, and flattened ceiling. Septa are inclined. The ornamentation consists of big granules at the polar zone with radial filaments. The spiral growth is regular. The diameter of the proloculus is 0.140-0.180mm (mean 0.160mm). Table I.3 sumarizes the biometric data of this species in the Miralles-La Tossa composite section.

Remarks. *Nummulites* aff. *incrassatus ramondiformis* from sample LT005 (Figs. I.8, 1 to 5; I.13, 12 to 26) have a test and proloculus diameter of smaller size than the *Nummulites incrassatus* (Fig. I.8, 6 to 9) from the Boro-Granella section (Priabona area, Roveda, 1961) and the *Nummulites incrassatus ramondiformis* (Fig. I.8, 10 to 14) from Cunial-Santa Giustina-Col dell'Asse section (Possagno area, Herb and Hekel, 1975). *Nummulites incrassatus incrassatus* (Fig. I.8, 15) illustrated by Herb and Hekel (1975) have a greater size of the test and the diameter of the proloculus than the specimens from the Tossa Formation. Thus, we use the terminology affinis because we consider the specimens from the Tossa Formation (sample LT005) as a primitive chronospecies within the lineage *Nummulites incrassatus ramondiformis*.

REFERENCES

Costa, E., Garcés, M., López-Blanco, M., Beamud, E., Gómez-Paccard, M., Larrasoaña, J.C., 2010. Closing and continentalization of the South Pyrenean foreland Basin (NE Spain): Magnetochronological constraints. Basin Research, 22(6), 904-917. DOI: 10.1111/j.1365-2117.2009.00452.x

Herb, R., Hekel, H., 1973. Biostratigraphy, Variability and Facies Relations of some Upper Eocene Nummulites from Northern Italy. Eclogae geologicae Helvetiae, 55(2), 419-445.

Herb, R., Hekel, H., 1975. Nummulites aus dem Obereocaen von Possagno. Schweizerische Paläontologische Abhandlungen, 97, 113-211.

Luciani, V., Negri, A., Bassi, D., 2002. The Bartonian-Priabonian transition in the Mossano section (Colli Berici, north-eastern Italy): a tentative correlation between calcareous plankton and shallow-water benthic zonations. Geobios, 35(1, Supplement), 140-149. DOI: 10.1016/S0016-6995(02)00055-4

Papazzoni, C.A., 1998. Biometric analysis of *Nummulites "ptukhiani"* (Z.D. KACHAREVA 1969) and *Nummulites fabianii* (Prever in FABIANI, 1905). Journal of Foraminiferal Research, 28(3), 161-176.

Papazzoni, C.A., Sirotti, A., 1995. Nummulite biostratigraphy at the Middle/Upper Eocene boundary in the northern Mediterranean area. Rivista Italiana di Paleontologia e Stratigrafia, 101(1), 63-80.

Roveda, V., 1961. Contributo allo studio di alcuni macroforaminiferi di Priabona. Rivista Italiana di Paleontologia, 67(2), 153-225.

Schaub, H., 1981. Nummulites et Assilines de la Tethys Paléogène. Taxonomie, phylogénèse et biostratigraphie. Mémoires suisses de Paléontologie, 104-106, 1-236.

Serra-Kiel, J., Reguant, S., 1984. Paleoecological conditions and morphological variation in monospecific banks of Nummulites: an example. Benthos'83, 2nd International Symposium on Benthic Foraminifera. Bulletin des Centres de Recherches Exploration-Production Elf-Aquitanie, 6, 557-563.

Serra-Kiel, J., Mató, E., Saula, E., Travé, A., Ferràndez-Cañadell, C., Busquets, P., Samsó, J.M., Tosquella, J., Barnolas., A., Àlvarez-Pérez, G., Franquès, J., Romero, J., 2003a. An inventory of the marine and transitional Middle/Upper Eocene deposits of the Southeastern Pyrenean Foreland Basin (NE Spain). Geologica Acta, 1(2), 201-229. DOI: 10.1344/105.000001610

Serra-Kiel, J., Travé, A., Mató, E., Saula, E., Ferràndez-Cañadell, C., Busquets, P., Tosquella, J., Vergés, J., 2003b. Marine and Transitional Middle/Upper Eocene Units of the Southeastern Pyrenean Foreland Basin (NE Spain). Geologica Acta, 1(2), 177-200. DOI: 10.1344/105.000001609

Teixell, A., Serra-Kiel, J., 1988. Sedimentología y distribución de foraminíferos en medios litorales y de plataforma mixta (Eoceno Medio y Superior, Cuenca del Ebro Oriental). Boletín Geológico y Minero, 94, 871-885.

Vanova, M., 1972. Nummulites from the area of Bojnice, the Upper Hron Depression, and the Budín Paleogene around Stúrovo. Zbornlk Geologickych vied Západné Karpaty, 17, 5-104.

TABLE I.3 Biometric data of 14 specimens of A- and B-Forms of Nummulites aff. incrassatus ramondiformis from sample LT005

Dimensions of the B-Form in mm (4 specimens measured)						
	Max	Min	Mean			
Diameter	4.90	3.85	4.37			
Equatorial section (mean values)						
Whorld	1	2	3	4	5	6
Radius	0.20	0.47	0.75	1.15	1.60	2.00
Chambers	13	13	17	22	24	29
Dimensions of the A-Form in mm (10 specimens measured)						
	Max	Min	Mean			
Diameter	2.70	2.20	2.50			
Equatorial section (mean values)						
Whorld	1	2	3	4	5	
Radius	0.25	0.50	0.70	1.00	1.35	
Chambers	5-6	13	18	20	22	

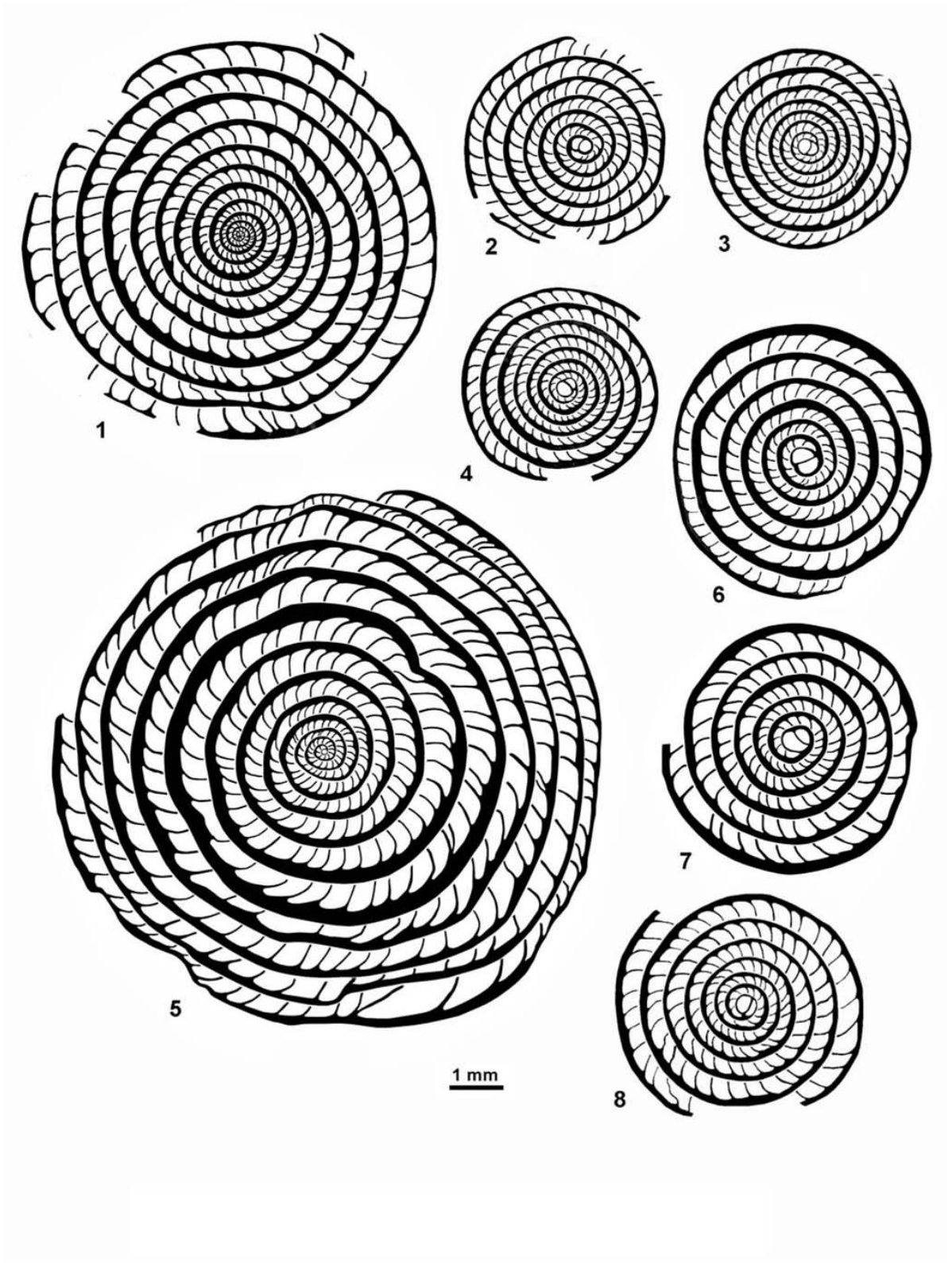

FIGURE I.2 Drawings of *Nummulites beaumonti* D'ARCHIAC and HAIME 1853 and *N. biarritzensis* D'ARCHIAC and HAIME 1853 from the Miralles-La Tossa composite section. 1-4) *N. beaumonti*. 1: B-Form from sample MM008; 2: A-Form from sample MM008; 3-4: A-Forms from sample MM022. 5-8) *N. biarritzensis*. 5: B-Form from sample MM004; 6-7: A-Forms from sample MM004; 8: A-Form from sample MM022.

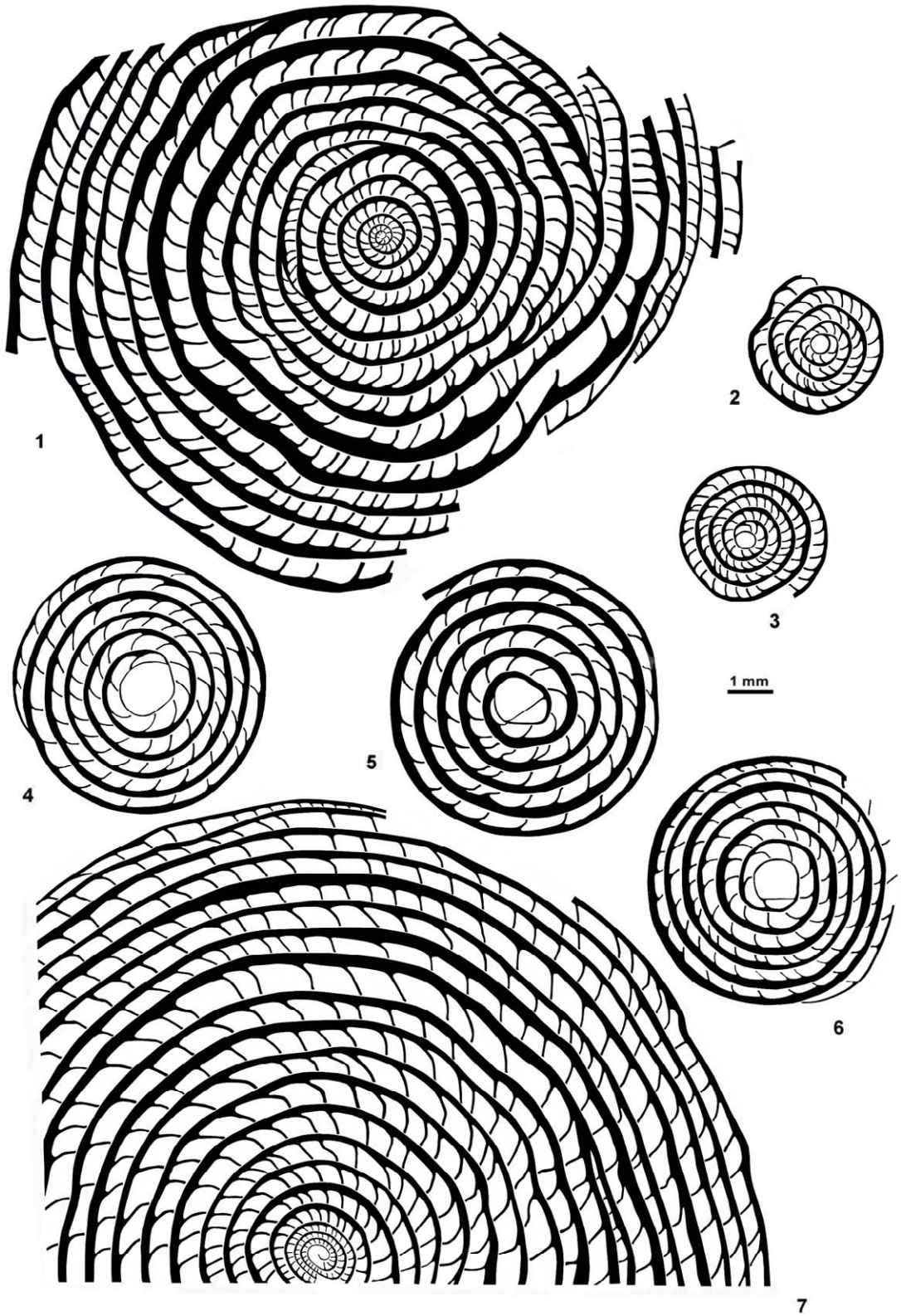

FIGURE I.3 | Drawings of *Nummulites hottingeri* SCHAUB 1981 and *Nummulites perforatus* DE MONTFORT 1808 from the Miralles-La Tossa composite section. 1-3) *N. hottingeri*. 1: B-Form from sample MM004; 2-3: A-Forms from sample MM022. 4-7) *N. perforatus*. 4-6: A-Forms from sample BM010; 7: B-Form from sample BM010.

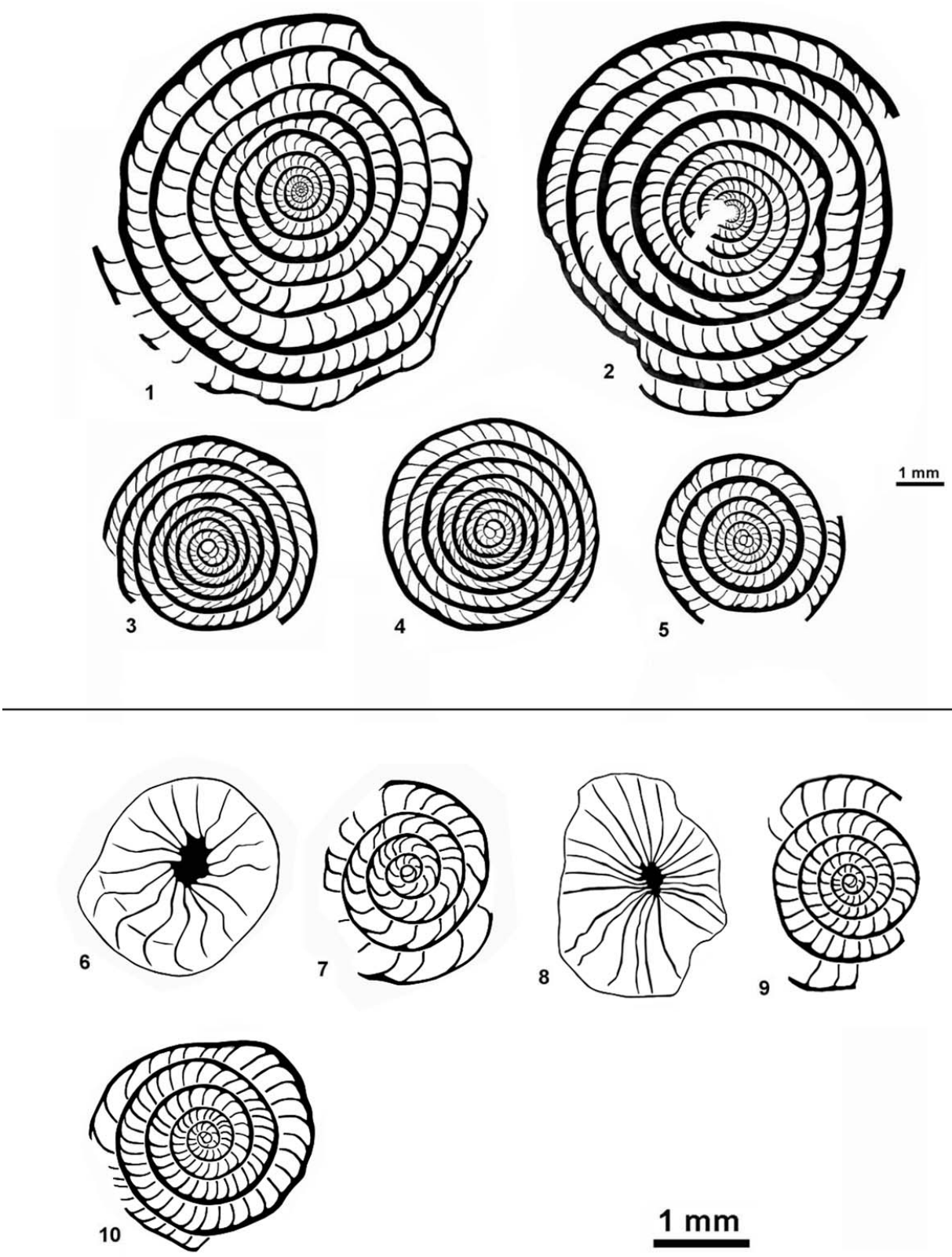

FIGURE I.4 | Drawings of *Nummulites vicaryi* D'ARCHIAC and HAIME 1853, *Nummulites stellatus* ROVEDA 1961 and *Nummulites orbignyi* GALEOTTI 1837 from the Miralles-La Tossa composite section. 1-5) *N vicaryi*. 1-2: B-Forms from sample MM028-29; 3-5: A-Forms from sample MM028-29. 6-9) *N. stellatus*. 6-7: A-Forms from sample LT000; 8-9: A-Forms from sample LT104. 10) *N. orbignyi*. 10: A-Form from sample LT157.

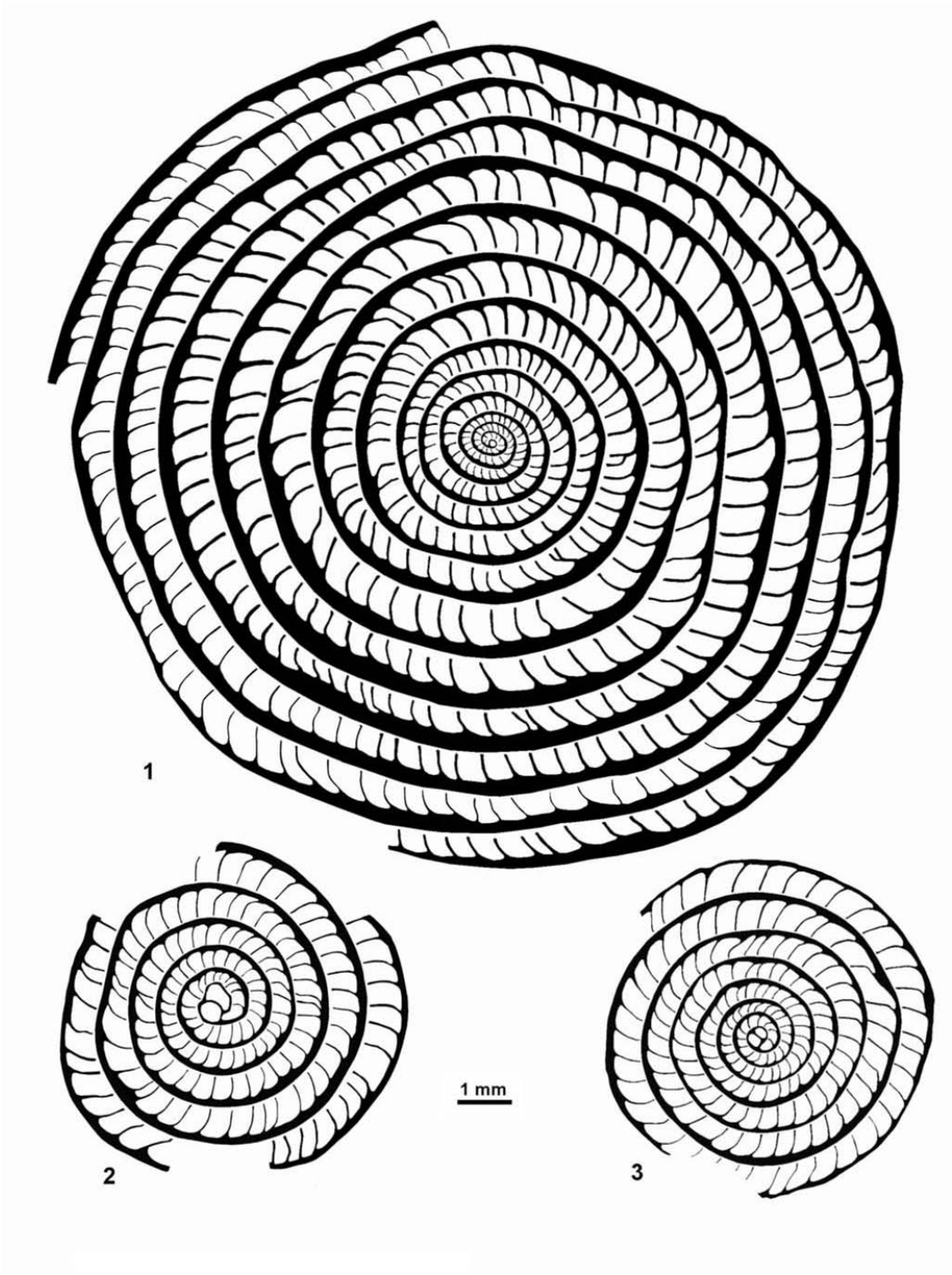

FIGURE I.5 Drawings of *Nummulites striatus* BRUGUIÈRE 1792 from the Miralles-La Tossa composite section. 1) B-Form from sample LT104; 2) A-Form from sample MM050; 3) A-Form from sample LT104.

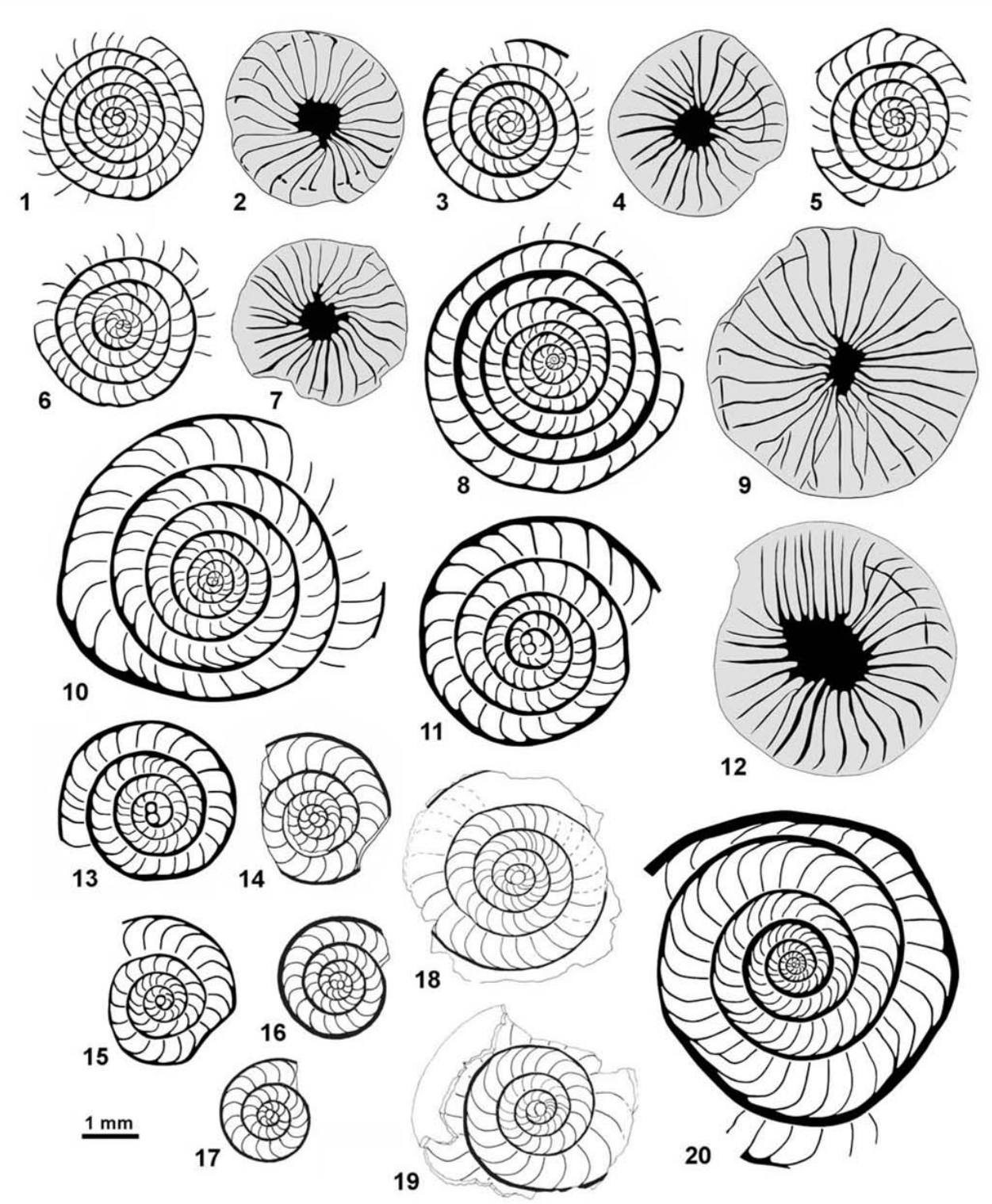

FIGURE I.6 | Drawings of *Nummulites chavannesi* DE LA HARPE 1978. 1-9) *N. chavannesi* from the sample LT005 in the Miralles-La Tossa composite section. 1, 3, 5, 6: A-Form equatorial sections; 2, 4, 7: A-Form external views; 8-9: equatorial section and external view respectively of a B-Form. 10-13) drawings after Roveda (1961) of *N. chavannesi* from the Boro-Granella section in the Priabona area. 10: B-Form equatorial section; 11, 13: A-Form equatorial sections; 12: B-Form external view. 14-20) drawings after Herb and Hekel (1975) of *N. chavannesi* from the Cunial-Santa Giustina-Col dell'Asse section in the Possagno area. 14-17: equatorial section of A-Forms from the Marne di Possagno Formation; 18: equatorial section from Calcare di Santa Giustina Formation; 19: equatorial section of A-Form from the Marne siltose Formation; 20: equatorial section of B-Form from the Marne siltose Formation.

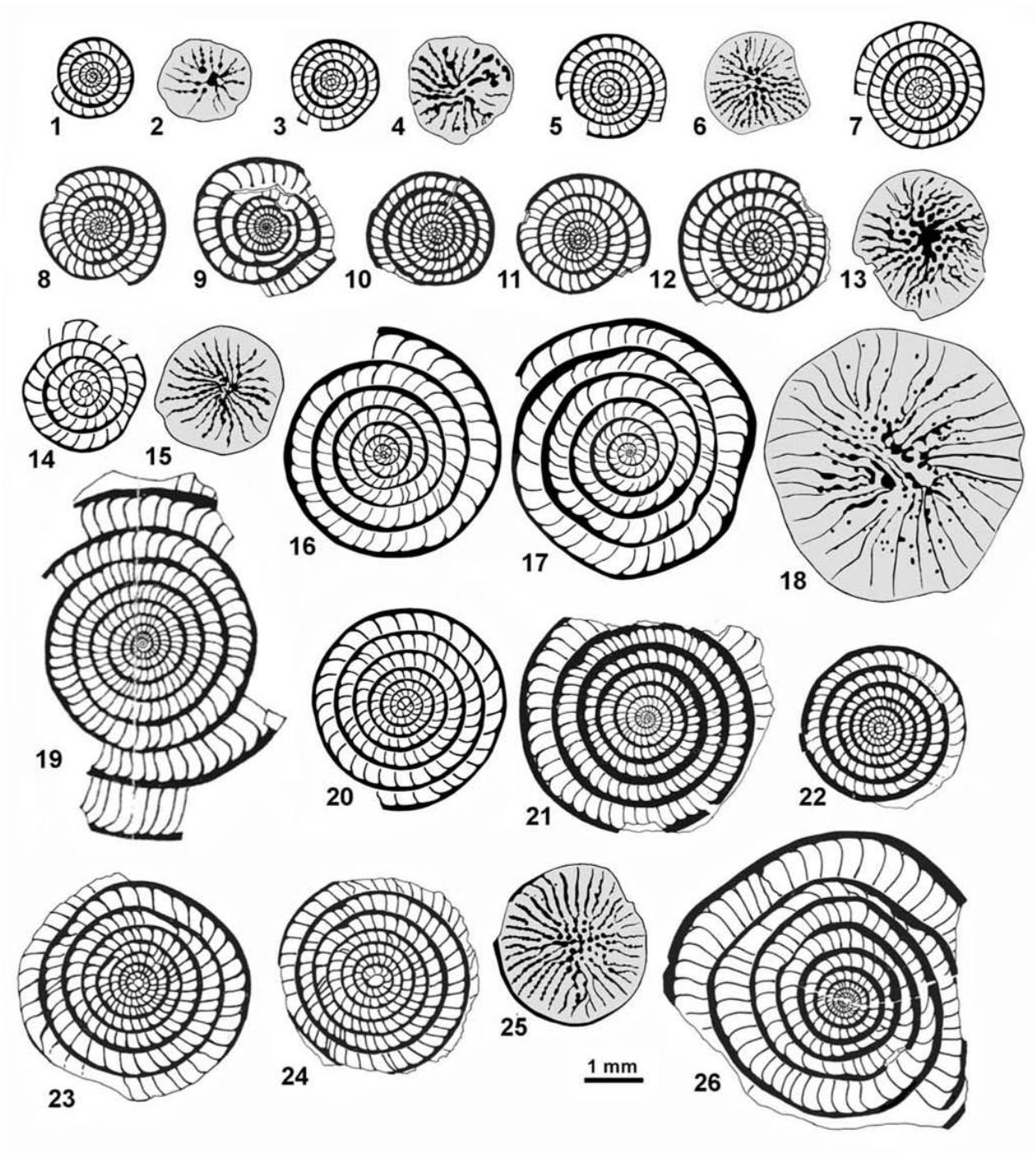

FIGURE I.7 | Drawings of 1-4) *Nummulites praegarnieri* SCHAUB 1981; 5-7, 14-18) *N. garnieri sturi* VANOVA 1972; 8-13, 21-22) *N. garnieri garnieri* DE LA HARPE in BOUSSAC 1911; 19-20) *N. garnieri* DE LA HARPE in BOUSSAC 1911; and 23-26) *N. garnieri inaequalis* HERB and HEKEL 1973. 1-2: *Nummulites praegarnieri* from sample BM005 in the Collbàs Formation (Miralles-La Tossa composite section); 1: A-Form equatorial section; 2: A-Form external view. 3-4: *Nummulites praegarnieri* from the Collbàs Formation. Holotype drawings after Schaub (1981); 3: A-Form equatorial section; 4: A-Form external view. 5-7: *Nummulites garnieri sturi* from the Upper Hron depression (Slovakia). Figure drawings after Vanova (1972); 5: equatorial section of the holotype; 6: external view of the holotype; 7: A-Form equatorial section. 8-13: *Nummulites garnieri garnieri* from the Marne di Possagno in Cunial-Santa Giustina-Col dell'Asse section (Possagno area, Italy). Figure drawings after Herb and Hekel (1975); 8-12: A-Form equatorial sections; 13: A-Form external view. 14-18: *Nummulites garnieri sturi* from sample LT005 in the Tossa Formation (Miralles-La Tossa composite section); 14: A-Form equatorial section; 15: A-Form external view; 16-17: B-Form equatorial sections; 18: B-Form external view. 19-20: *Nummulites garnieri* from Châteaugarnier (western Alps, France). Figure drawings after Schaub (1981); 19: B-Form equatorial section; 20: A-Form equatorial section. 21-22: *Nummulites garnieri garnieri* from Châteaugarnier (western Alps, France); Figure drawings after Herb and Hekel (1973); 21: B-Form equatorial section; 22: A-Form equatorial section. 23-26: *Nummulites garnieri inaequalis* from the Marne siltose in Cunial-Santa Giustina-Col dell'Asse section (Possagno section, Italy). Figure drawings after Herb and Hekel (1975); 23-24: A-Form equatorial sections; 25: A-Form external view; 26: B-Form equatorial section.

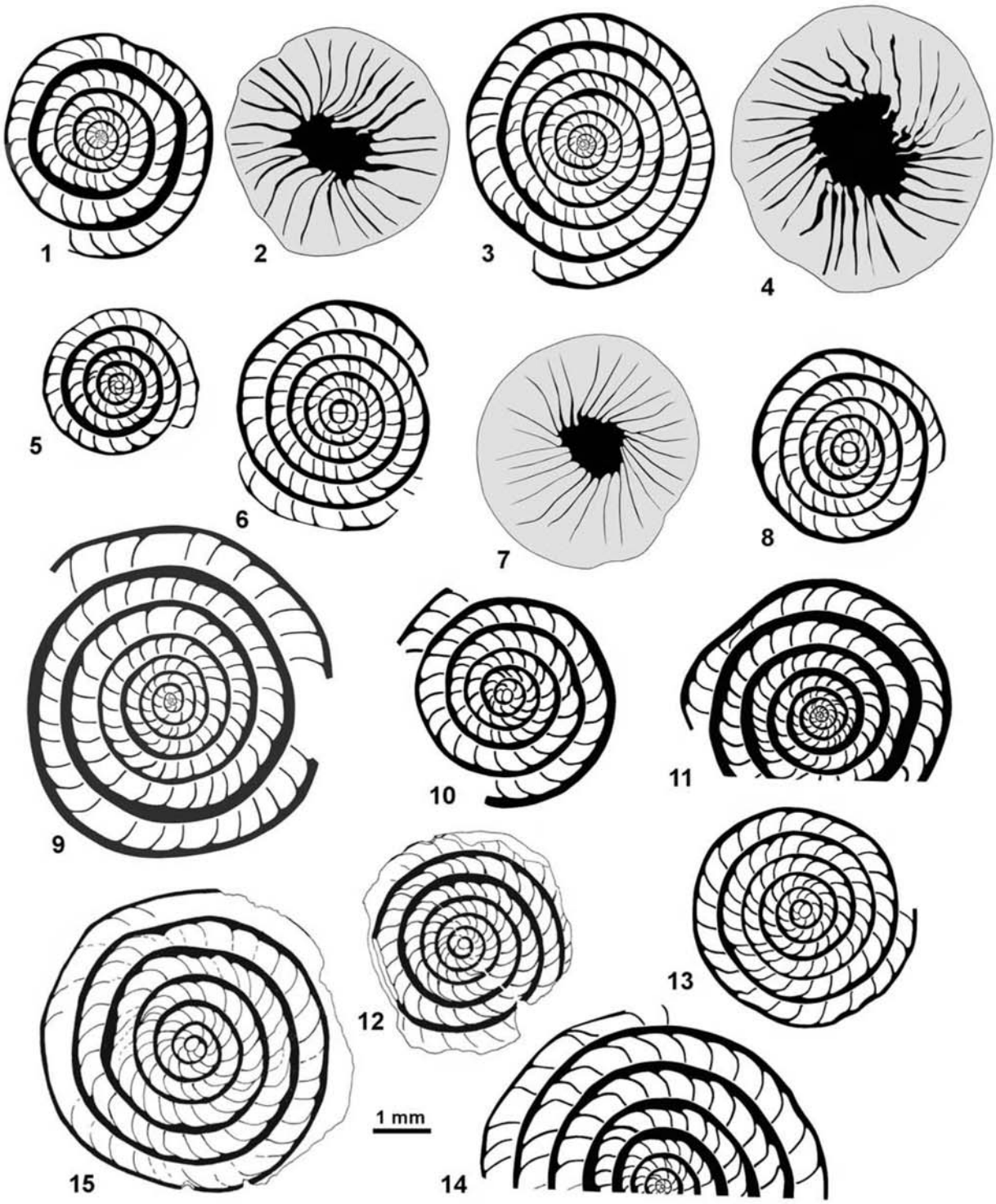

FIGURE I.8 | Drawings of 1-5) *Nummulites* aff. *incrassatus ramondiformis* DE LA HARPE in ROZLOZSNIK 1926, 6-9) *N. incrassatus* DE LA HARPE 1883, 10-14) *N. incrassatus ramondiformis* DE LA HARPE in ROZLOZSNIK 1926, and 15) *N. incrassatus incrassatus* DE LA HARPE 1883. 1-5: *N.* aff. *incrassatus ramondiformis* from sample LT005 in the Miralles-La Tossa composite section; 1, 3: B-Form equatorial sections; 2, 4: B-Form external views; 5: A-Form equatorial section. 6-9: drawings after Roveda (1961) of *N. incrassatus* from the Boro-Granella section in the Priabona area; 6, 8: A-Form equatorial sections; 7: A-Form external view; 9: B-Form equatorial section. 10-14: drawings after Herb and Hekel (1975) of *N. incrassatus ramondiformis* from the Cunial-Santa Giustina-Col dell'Asse section in the Possagno area; 10: A-Form equatorial section from the Marne di Possagno; 11: B-Form equatorial section from the Marne di Possagno; 12: equatorial section of an A-Form from the Calcaria di Santa Giustina; 13: equatorial section of an A-Form from the Marne siltose Formation; 14: equatorial section of a B-Form from the Marne siltose Formation. 15: a drawing after Herb and Hekel (1975) of an A-Form equatorial section of an *N. incrassatus incrassatus* from the Cunial-Santa Giustina-Col dell'Asse section in the Possagno area.

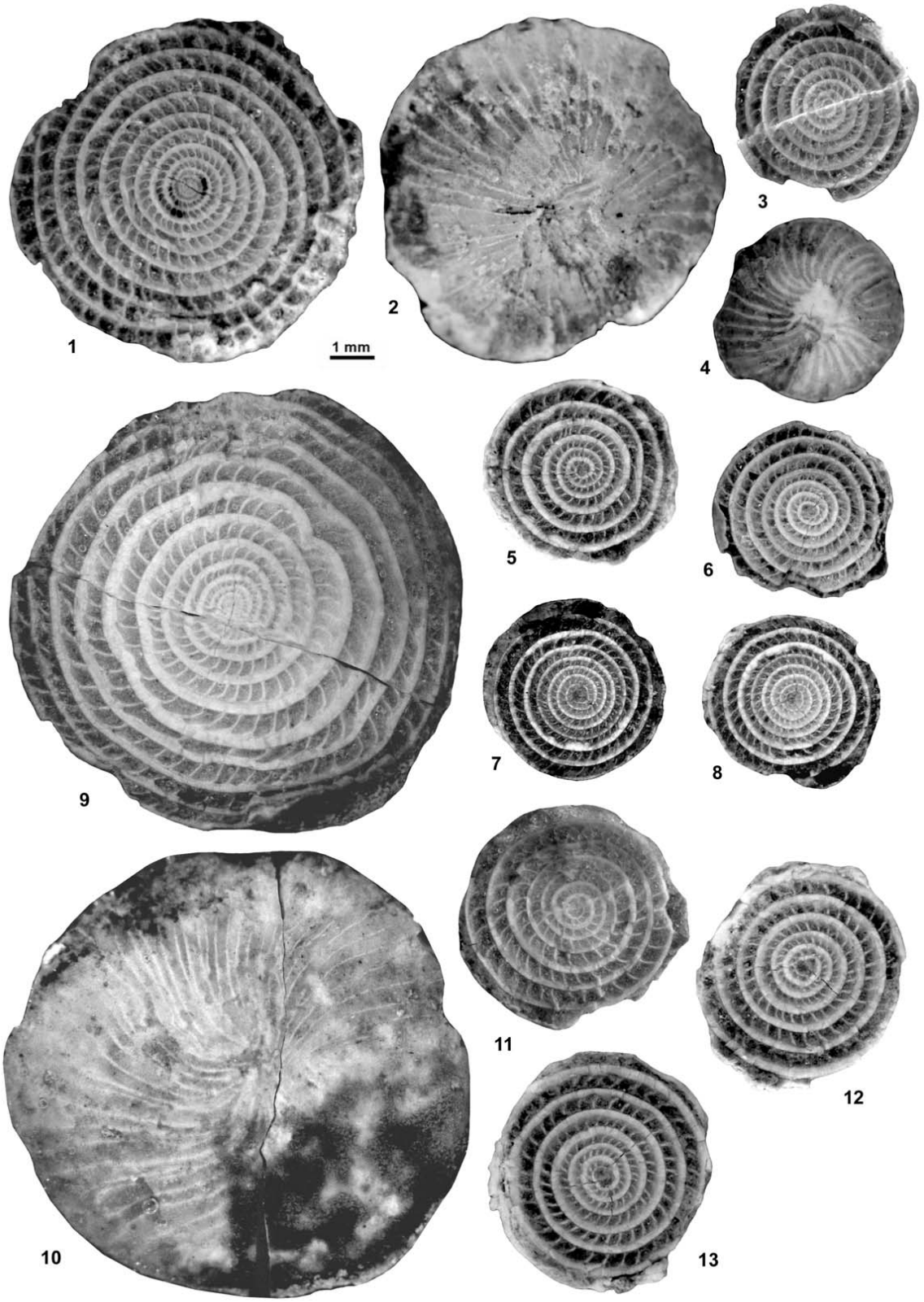

FIGURE I.9 | *Nummulites beaumonti* D'ARCHIAC and HAIME 1853 and *N. biarritzensis* D'ARCHIAC and HAIME 1853 from the Miralles-La Tossa composite section. 1-8) *N. beaumonti*. 1-2: B-Forms from sample MM008; 3-6: A-Forms from sample MM008; 7-8: A-Forms from sample MM022. 9-13) *N. biarritzensis*. 9-10: B-Form from sample MM004; 11-12: A-Forms from sample MM004; 13: A-Form from sample MM022.

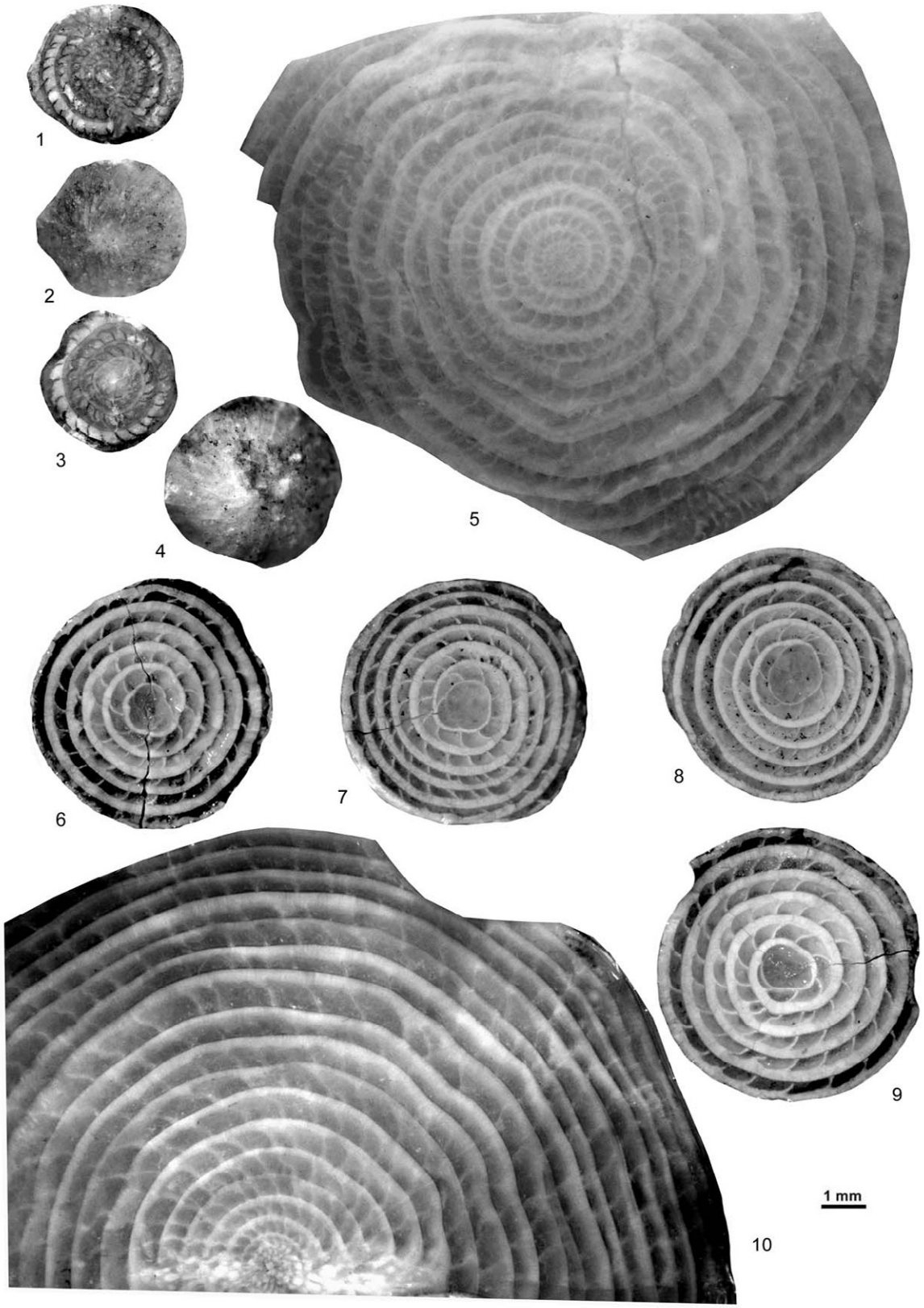

FIGURE I.10 *Nummulites hottingeri* SCHAUB 1981 and *Nummulites perforatus* DE MONTFORT 1808 from the Miralles-La Tossa composite section. 1-5) *N. hottingeri*. 1-4: A-Forms from sample MM022; 5: B-Form from sample MM004. 6-10) *N. perforatus*. 6-9: A-Forms from sample BM010; 10: B-Form from sample BM010.

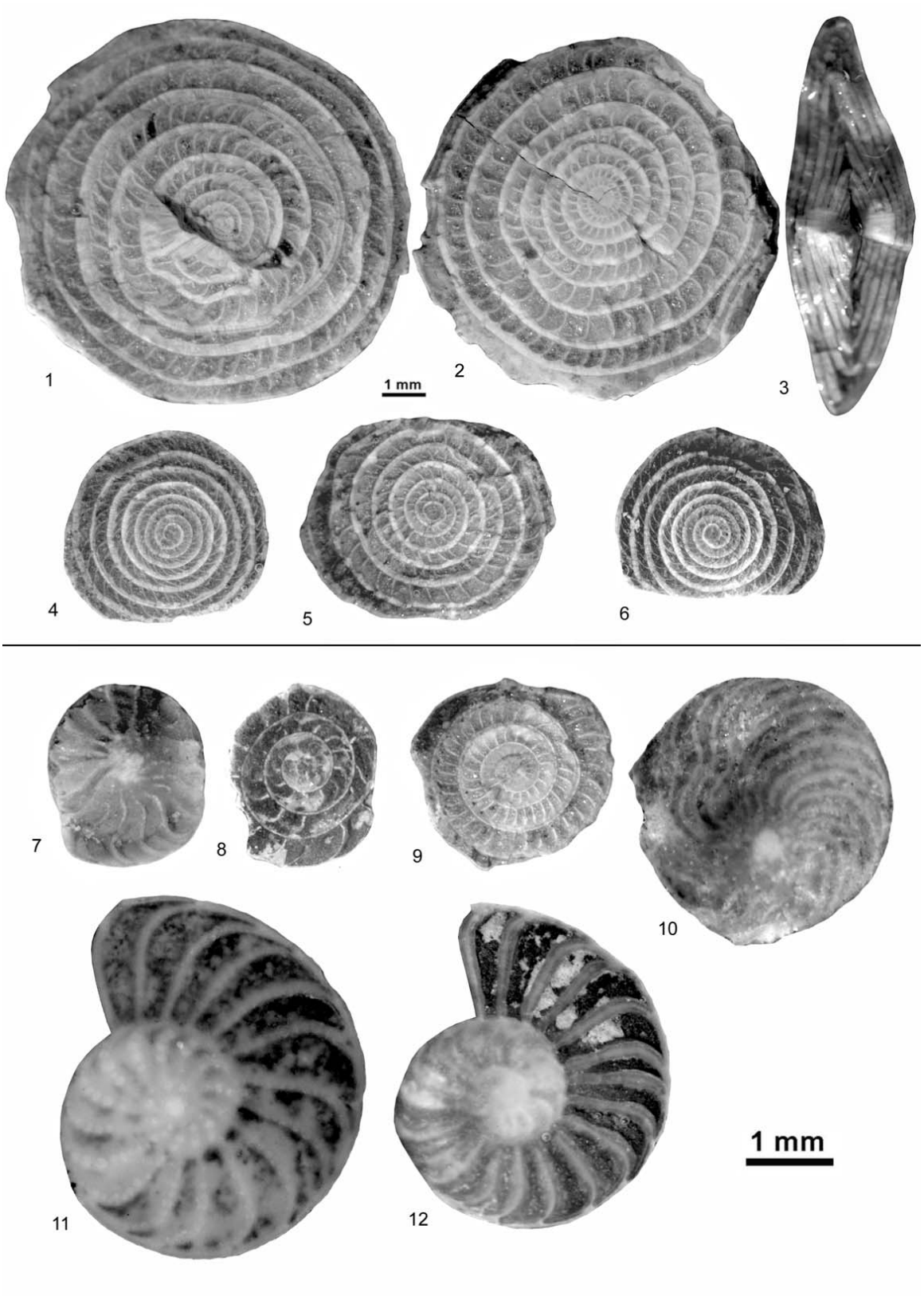

FIGURE I.11 *Nummulites vicaryi* D'ARCHIAC and HAIME 1853, *Nummulites stellatus* ROVEDA 1961, *Nummulites orbignyi* GALEOTTI 1837, *Operculina roselli* HOTTINGER 1977 and *Assilina schwageri* SILVESTRI 1928 from the Miralles-La Tossa composite section. 1-6) *N. vicaryi*. 1-3: B-Forms from sample MM028-29; 4-6: A-Forms from sample MM028-29. 7-8) *N. stellatus*. 7-8: A-Forms from sample LT000. 9) *N. orbignyi*. A-Form from sample LT157. 10) *O. rosella*. A-Form from sample MM024. 11-12) *A. schwageri*. 11-12: A-Forms from sample MM008.

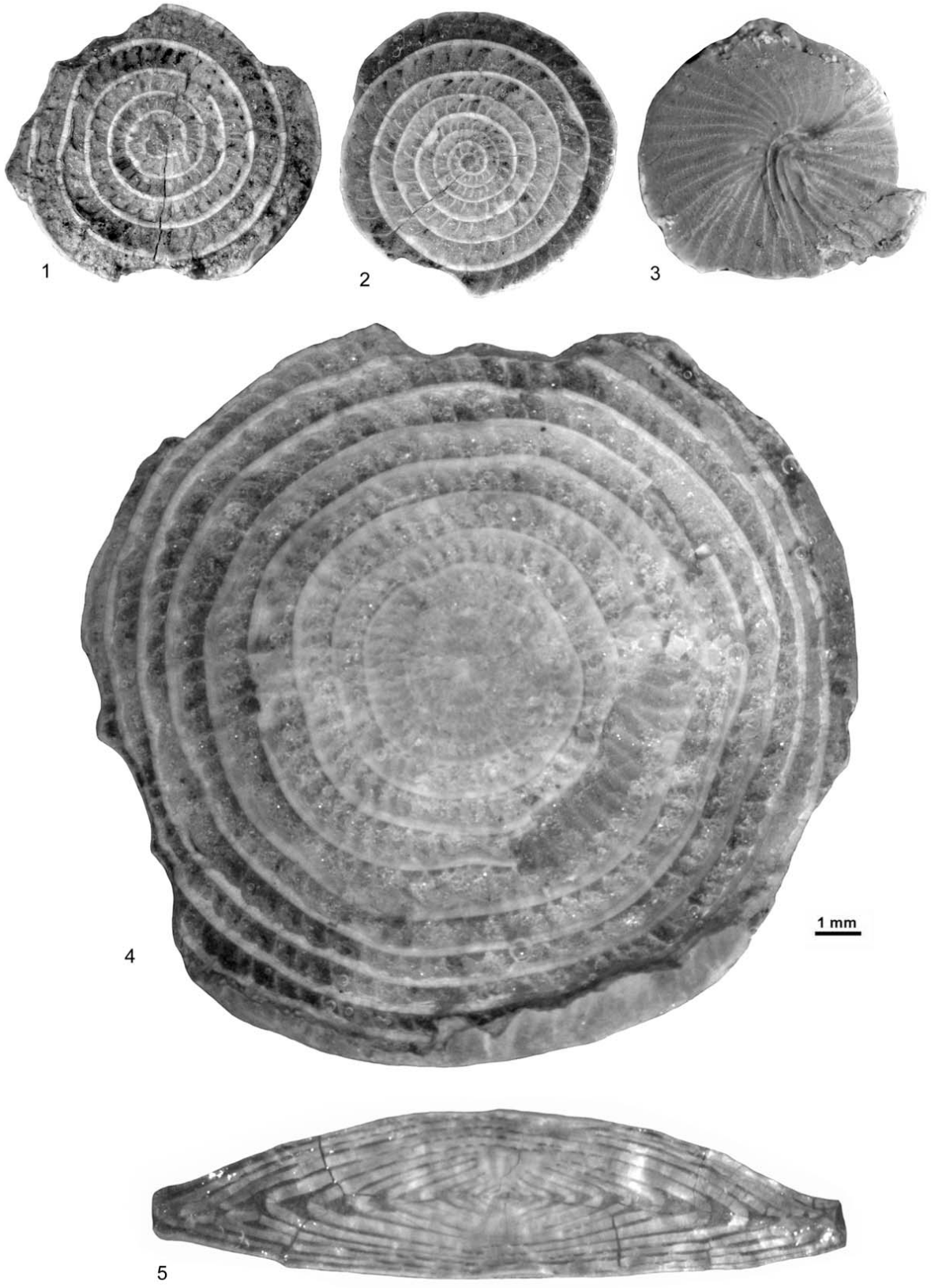

FIGURE I.12 *Nummulites striatus* BRUGUIÈRE 1792 from the Miralles-La Tossa composite section. 1, 3) A-Forms from sample MM050; 2) A-Form from sample LT104; 4-5) B-Forms from sample LT104.

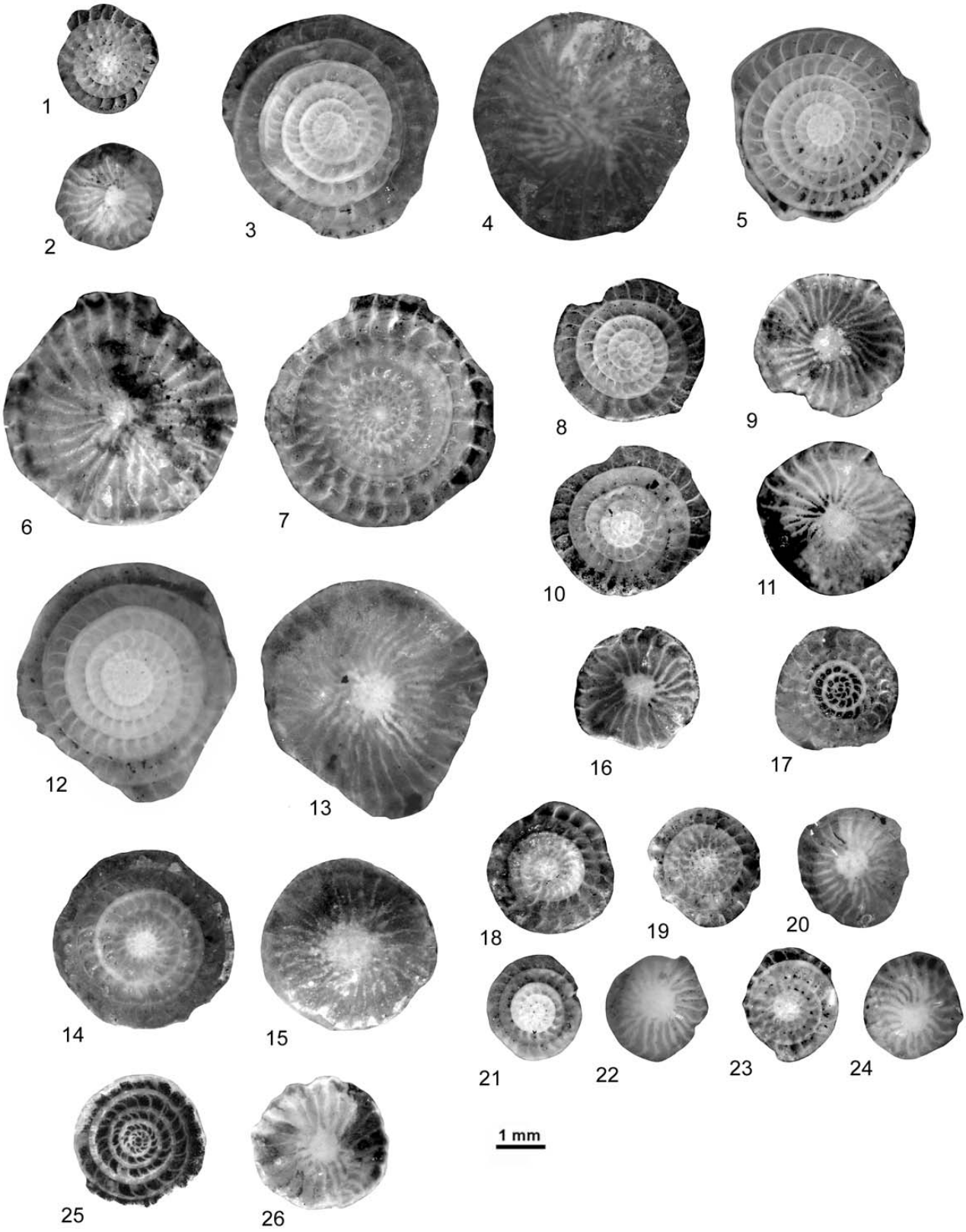

FIGURE I.13 *Nummulites garnieri sturi* VANOVA 1972, *Nummulites chavannesi* DE LA HARPE 1978, *Nummulites* aff. *incrassatus ramondiformis* DE LA HARPE in ROZLOZSNIK 1926 from the Miralles-La Tossa composite section. 1-5) *N. garnieri sturi*. 1-4: A-Forms from sample LT005; 5: B-Form from sample LT005. 6-11) *N. chavannesi*. 6-7: B-Forms from sample LT005; 8-11: A-Forms from sample LT005. 12-26) *N.* aff. *incrassatus ramondiformis*. 12-15: B-Forms from sample LT005; 16-26: A-Forms from sample LT005.

TABLE II | Results of the calcareous nannofossil quantitative analysis of the Miralles-La Tossa composite section. PDE: preservation degree of the assemblage; PRA: presence of reworked assemblages; TSA: total species abundance in number of specimens per field of view; and RASS: relative abundance of single species (%). Indidiual and total abundance of nannofossil: A (abundant) more than 20 specimens per field of view (spp/fv); C (common) 10-20spp/fv; F (few) 1-10spp/fv; R (rare) 0,1-1spp/fv; P (presence) less than 0,1spp/fv; B (barren of nannofossils). Preservation degree and reworked assemblages: G (good) individual specimens exhibit little or no dissolution or overgrowth, diagnostic characteristics are preserved, and nearly all of the species can be identified; M (moderate) individual specimens show evidence of dissolution or owergrowth, some specimens cannot be identified to species level; P (poor) individual specimens exhibit considerable dissolution or overgrowth, many specimens cannot be identified to species level

Formations	Sample	meters	Total abundance	Preservation	Reworking	*Braarudosphaera bigelowii*	*Bramletteius serraculoides*	*Calciduscus protoannulus*	*Calciduscus spp.*	***Chiasmolithus grandis***	***Chiasmolithus oamaruensis***	*Chiasmolithus spp.*	*Coccolithus formosus*	*Coccolithus pelagicus*	*Coronocyclus bramlettei*	*Cyclicargolithus floridanus*	***Dictyococcites bisectus***	*Dictyococcites scrippsae*	*Discoaster barbadiensis*	*Discoaster saipanensis*	*Discoaster tani*	*Heliosphaera spp.*	***Isthmolithus recurvus***	*Lanternitus minutus*	*Pemma basquensis*	*Pemma papillatum*	*Pemma spp.*	*Pontosphaera spp.*	*Postosphaera exilis*	*Postosphaera multipora*	*Reticulofenestra dyctioda*	*Reticulofenestra reticulata*	*Reticulofenestra spp.*	*Reticulofenestra umbilicus*	*Sphenolithus cf. anharropus*	*Sphenolithus morjormis*	***Sphenolithus obtusus***	*Zygrhablithus bijugatus*	NANNOFOSSIL ZONES
TOSSA FORMATION	LT034	1345.1	B	-	-	-	-	-	-	-	-	-	-	-	-	-	-	-	-	-	-	-	-	-	-	-	-	-	-	-	-	-	-	-	-	-	-	-	-	-
	LT031	1322.1	B	-	-	-	-	-	-	-	-	-	-	-	-	-	-	-	-	-	-	-	-	-	-	-	-	-	-	-	-	-	-	-	-	-	-	-	-	-
	LT027	1302.7	B	-	-	-	-	-	-	-	-	-	-	-	-	-	-	-	-	-	-	-	-	-	-	-	-	-	-	-	-	-	-	-	-	-	-	-	-	-
	LT020	1275.8	B	-	-	-	-	-	-	-	-	-	-	-	-	-	-	-	-	-	-	-	-	-	-	-	-	-	-	-	-	-	-	-	-	-	-	-	-	-
	LT016	1266.6	B	-	-	-	-	-	-	-	-	-	-	-	-	-	-	-	-	-	-	-	-	-	-	-	-	-	-	-	-	-	-	-	-	-	-	-	-	-
	LT014	1261.3	B	-	-	-	-	-	-	-	-	-	-	-	-	-	-	-	-	-	-	-	-	-	-	-	-	-	-	-	-	-	-	-	-	-	-	-	-	-
	LT012	1253.3	B	-	-	-	-	-	-	-	-	-	-	-	-	-	-	-	-	-	-	-	-	-	-	-	-	-	-	-	-	-	-	-	-	-	-	-	-	-
	LT010	1248.1	B	-	-	-	-	-	-	-	-	-	-	-	-	-	-	-	-	-	-	-	-	-	-	-	-	-	-	-	-	-	-	-	-	-	-	-	-	-
	LT009	1246.1	B	-	-	-	-	-	-	-	-	-	-	-	-	-	-	-	-	-	-	-	-	-	-	-	-	-	-	-	-	-	-	-	-	-	-	-	-	-
	LT007	1241.4	B	-	-	-	-	-	-	-	-	-	-	-	-	-	-	-	-	-	-	-	-	-	-	-	-	-	-	-	-	-	-	-	-	-	-	-	-	-
IGUALADA FORMATION	LT005	1237.5	P	P	-	-	-	-	-	-	-	-	-	P	-	-	-	P	P	-	-	-	-	-	-	-	-	-	-	-	-	P	P	-	-	-	-	-	-	-
	LT001	1225.8	F	M	-	-	-	-	-	-	-	-	P	P	-	-	-	F	R	-	-	-	P	-	-	-	-	-	-	-	-	F	-	P	-	-	P	-	-	-
	LT168	1226.0	P	P	-	-	-	-	-	-	-	-	-	P	-	-	-	P	P	-	-	-	-	-	P	-	-	-	-	-	-	P	P	-	-	-	-	-	-	-
	LT164	1212.0	R	P	-	-	-	-	-	-	-	-	-	-	-	-	-	R	R	R	P	-	-	-	-	-	-	-	-	-	-	F	R	P	-	-	-	-	-	-
	LT160	1199.5	F	P	-	-	-	P	-	-	cf.	-	R	R	-	-	-	F	F	R	-	-	-	-	P	-	-	-	-	-	-	R	P	R	-	-	-	-	-	R
	LT155	1124.7	R	P	-	-	-	-	-	-	-	-	P	R	-	-	-	R	R	-	-	-	-	-	-	-	-	-	-	-	-	-	P	-	-	-	-	-	-	P
	LT151	1104.4	F	M	-	-	-	-	-	-	-	-	-	F	-	-	-	F	R	cf.	P	-	-	-	P	-	-	-	-	-	-	F	R	R	-	-	-	-	-	-
	LT146	1090.2	F	P	P	-	-	-	-	-	-	-	-	-	-	-	-	F	R	R	P	-	-	-	-	-	-	-	-	-	-	C	-	F	-	-	-	-	-	-
	LT141	1074.5	F	M	-	-	-	-	-	-	-	-	R	R	-	-	-	F	R	-	-	-	P	P	-	-	-	-	-	-	-	F	R	F	-	-	-	-	-	-
	LT138	1066.0	C	G	-	-	-	-	-	-	P	-	R	F	-	-	-	R	F	P	-	-	P	-	-	-	-	-	-	-	-	F	-	F	-	-	-	-	-	R
	LT135	1057.2	F	M	-	-	-	-	-	-	-	-	R	R	-	-	-	F	F	-	-	-	-	-	-	-	-	-	-	-	-	R	-	F	-	-	-	-	-	P
	LT131	1042.7	C	G	-	-	-	P	P	-	-	-	R	F	-	-	-	F	F	-	-	-	P	-	-	-	-	-	-	-	-	C	P	F	-	-	-	-	-	-
	LT128	1032.0	C	M	-	-	-	-	-	-	P	P	P	F	-	-	-	F	F	P	P	P	P	-	R	-	-	-	-	-	-	C	-	F	-	-	-	-	-	-
	LT126	979.8	F	G	P	-	-	-	-	-	-	-	P	F	-	-	-	F	F	P	P	P	P	-	-	-	-	-	-	-	-	F	R	F	-	-	-	-	-	-
	LT123	969.1	P	M	-	-	-	-	-	-	-	P	-	-	-	-	-	P	-	-	-	-	P	-	-	-	-	-	-	-	-	F	P	P	-	-	-	-	-	-
	LT121	959.6	C	M	P	-	-	-	-	-	R	P	-	R	F	-	-	R	R	-	-	-	P	-	-	-	-	-	-	-	-	F	P	R	-	-	-	-	-	-
	LT118	948.0	F	M	-	-	-	-	-	-	-	-	-	P	-	-	-	R	R	-	-	-	-	-	-	-	-	-	-	-	-	R	P	-	-	-	-	-	-	-
	LT115	937.3	C	G	P	-	-	P	-	-	R	-	-	R	R	-	-	F	R	R	P	-	-	-	P	-	-	-	-	-	-	F	-	R	-	-	-	-	-	-
	LT111	919.5	F	G	P	-	-	-	-	-	-	-	-	R	R	-	-	R	R	P	-	-	-	-	P	-	-	-	-	-	-	F	-	R	-	-	-	-	-	-
	LT108	911.3	F	M	-	-	-	P	-	-	-	-	P	R	R	-	-	R	F	-	P	-	P	P	-	-	-	-	-	-	-	R	P	R	-	-	-	-	-	P
	LT105	903.4	C	G	P	-	-	R	-	-	R	-	-	R	F	-	-	F	F	-	P	-	-	-	-	-	-	-	-	-	-	F	-	P	-	-	-	-	-	-
	LT104	901.3	C	M	-	-	-	-	-	-	P	-	-	R	F	-	-	R	R	-	-	-	-	-	R	-	-	-	-	-	-	F	-	R	-	-	-	-	-	R
	LT102	893.8	F	G	-	-	-	-	-	-	-	P	-	R	F	-	-	P	F	-	-	-	R	-	-	-	-	-	-	-	-	F	-	P	-	-	-	-	-	-
	LT101	884.1	C	G	-	-	-	-	-	-	R	-	-	R	R	-	-	F	R	R	R	-	P	P	-	-	-	-	-	-	-	F	-	P	-	-	-	-	-	-
	LT100	875.3	C	G	-	-	-	-	-	-	R	-	-	R	F	-	-	F	R	R	P	-	P	R	-	-	-	-	-	-	-	C	R	F	-	-	-	-	-	-
	MM028	703.5	P	P	-	-	-	-	-	-	-	-	-	-	-	-	-	P	-	-	-	-	-	-	-	-	-	-	-	-	-	P	P	-	-	-	-	-	-	-
	MM015	628.9	A	G	P	-	P	-	-	-	-	-	-	R	F	-	-	R	F	R	-	-	P	-	-	P	-	-	-	-	-	C	P	F	-	-	R	-	R	-
	MM014	624.5	C	G	P	-	-	P	-	-	-	-	-	R	F	cf.	-	R	F	-	R	-	-	P	-	-	-	-	-	-	-	F	P	R	-	-	R	R	P	-
	MM013	617.0	F	M	-	-	-	-	-	-	-	-	-	R	R	-	-	P	R	-	P	-	-	-	-	-	P	F	-	-	-	F	R	R	-	-	P	-	-	-
	MM012	610.0	A	G	P	-	-	-	-	-	P	-	-	R	F	-	-	R	F	R	-	-	-	-	-	P	-	-	-	-	-	C	P	F	-	-	R	R	-	-
	MM007	524.5	F	M	R	-	-	-	-	-	-	-	-	P	R	-	-	P	R	-	P	-	-	-	-	-	-	-	-	-	-	F	R	F	-	-	R	P	-	-
	MM004	509.8	F	M	P	-	-	-	-	-	-	-	-	-	F	-	-	P	F	P	P	-	-	-	-	-	P	-	-	-	-	F	R	R	-	-	-	-	-	-
	MM001	489.5	F	P	R	-	-	-	-	-	-	-	-	-	R	-	-	R	R	-	R	-	-	-	-	-	-	-	-	-	-	F	R	R	-	-	P	-	-	P
	BM010	470.2	B	-	-	-	-	-	-	-	-	-	-	-	-	-	-	-	-	-	-	-	-	-	-	-	-	-	-	-	-	-	-	-	-	-	-	-	-	-
	BM008	457.5	C	M	F	P	P	-	-	-	R	-	-	R	R	-	-	P	F	R	P	-	-	-	-	-	P	F	-	-	-	P	F	R	R	-	-	P	P	-
	BM005	446.0	F	P	F	P	-	-	-	-	-	-	-	P	R	-	-	F	-	P	-	-	P	-	P	-	-	-	-	-	-	-	R	P	R	-	-	-	-	-
	BM002	437.5	C	P	C	-	-	-	P	-	P	-	-	P	F	P	P	-	R	-	-	-	-	-	-	-	-	-	-	-	-	-	F	P	R	P	-	R	-	-

TABLE III | Magnetostratigraphic results. Characteristic remanent magnetization directions of the Miralles and La Tossa magnetostratigraphic sections. Site Nº, name and number of paleomagnetic site and specimen code; Stratigraphic level, stratigraphic position of the paleomagnetic site in the Miralles-La Tossa composite section; Dec. and Inc.: declination and inclination in geographic (in situ) and stratigraphic coordinates (after bedding correction); Dip. Az. and Dip.: azimuth of down dip direction of local bedding and dip angle of local bedding; Virtual Geomagnetic Pole Lat.: latitude of the Virtual Geomagnetic Pole used to build the local magnetostratigraphy of Miralles and La Tossa sections (see Fig. 6)

		Geographic coordinates		Stratigraphic coordinates				
Site Nº	Stratigraphic level (m)	Dec. (º)	Inc. (º)	Dec. (º)	Inc. (º)	Dip az. (º)	Dip. (º)	VGP Lat. (º)
Miralles Section								
CS001-1A	6.0	391.1	47.8	361.8	28.2	315	40	63.5
CS002-2A	13.6	435.7	58.5	366.5	56.2	315	40	83.1
CS003-1B	34.0	391.7	45.5	363.9	26.9	315	40	62.5
CS004-2B	46.3	340.7	67.5	325.2	29.3	315	40	50.5
CS006-2A	60.8	369.1	69.8	334.4	36.4	315	40	59.7
CS008-1A	73.3	326.3	-51.8	421.6	-81.8	315	40	-32.6
CS009-1B	81.0	315.6	-43.8	326.0	-83.7	315	40	-30.9
CS012-1A	99.3	301.3	-44.7	251.2	-80.1	315	40	-44.8
CS013-1C	108.8	215.1	-28.1	198.8	-16.0	315	40	-52.7
CS027-2A	110.3	284.7	-48.0	197.8	-52.0	330	60	-73.3
CS028-1C	113.5	223.3	-80.6	158.9	-27.1	330	60	-57.3
CS029-1A	120.0	297.8	-31.5	227.5	-63.4	330	60	-55.7
CS030-1A	126.8	282.0	-64.5	175.0	-45.0	330	60	-74.5
CS031-1A	144.8	341.5	-80.7	146.1	-39.0	330	60	-55.6
CS016-1D	150.8	232.1	-67.5	173.6	-25.1	330	60	-61.1
CS017-1B	151.5	305.6	-40.4	203.5	-68.5	330	60	-71.0
CS032-2B	151.8	260.9	-12.5	238.5	-25.3	330	60	-32.2
CS033-1A	161.5	264.8	-50.1	196.4	-38.9	330	60	-66.1
CS019-1B	162.3	301.4	-47.5	191.3	-62.7	330	60	-81.3
CS034-1C	168.0	304.5	-53.0	179.2	-61.0	330	60	-89.2
CS020-1B	168.3	299.4	-58.3	175.5	-55.3	330	60	-83.3
CS021-1B	172.5	298.2	-29.6	231.9	-63.6	330	60	-52.7
CS035-1C	173.4	251.0	-77.7	162.9	-31.9	330	60	-61.7
CS022-1B	176.8	132.7	31.5	408.2	76.2	330	60	54.6
CS022-2A	176.8	297.7	-14.9	259.7	-57.8	330	60	-31.1
CS023-2B	180.8	285.3	-62.4	176.7	-47.3	330	60	-76.7
CS036-1C	184.5	325.0	-41.4	162.6	-78.3	330	60	-62.3
CS024-1B	191.5	259.8	-67.9	174.3	-35.5	330	60	-67.6
CS037-1A	195.3	217.2	-27.4	204.5	3.0	330	60	-41.6
CS038-1C	203.0	260.8	-14.9	236.0	-26.3	330	60	-34.3
CS026-3C	210.0	223.4	-14.7	218.3	5.4	330	60	-33.8
CS039-1A	218.0	91.9	28.0	406.1	40.8	330	60	47.7
CS039-2A	218.0	449.3	51.3	374.9	41.7	330	60	68.6
CS042-1A	225.2	321.1	-46.8	166.0	-72.1	330	60	-72.0
CS043-2A	230.8	95.9	46.2	381.7	46.3	330	60	67.5
CS044-2B	244.5	448.2	21.4	412.6	35.5	330	60	40.6
CS045-1B	245.8	269.6	-52.8	192.8	-41.8	330	60	-69.6
CS045-1C	245.8	284.0	-41.5	208.5	-52.4	330	60	-65.9
CS047-1A	261.5	289.4	-61.9	175.8	-49.1	330	60	-78.0
CS049-1B	265.5	239.8	-14.4	226.7	-8.1	330	60	-34.0
CS051-1A	283.8	97.1	-25.9	101.7	15.4	330	60	-3.4
CS052-1A	286.8	420.9	19.1	403.0	11.3	330	60	37.7
CS053-1E	291.5	267.5	-51.1	195.1	-40.6	330	60	-67.8
CS056-1A	297.3	279.6	-48.2	198.4	-48.6	330	60	-70.9
CS057-1B	301.8	254.7	-11.6	236.3	-19.5	330	60	-31.7
CS058-2A	321.0	290.4	-25.9	246.6	-34.0	354	66	-29.6
CS060-2B	343.3	290.8	-20.9	252.6	-33.2	354	66	-24.8
CS060-1B	343.3	146.4	61.0	371.7	48.8	354	66	74.9
CS065-2A	348.5	412.0	35.0	398.1	-8.6	354	66	32.5
CS065-1B	348.5	367.7	50.6	362.5	-14.2	354	66	41.2
CS062-1A	351.3	442.2	66.5	378.1	21.7	354	66	55.8
CS062-1B	351.3	128.7	77.5	363.0	32.6	354	66	66.1
CS063-2A	357.3	198.1	66.2	338.6	44.8	354	66	66.8
CS064-1B	361.5	106.1	49.7	397.7	33.0	354	66	50.2
CS066-1A	362.5	233.8	62.1	322.9	34.5	354	66	51.3
CS067-2B	381.0	221.0	-37.8	206.4	4.8	347	60	-40.0
CS068-3A	392.4	194.1	-40.7	187.6	14.6	347	60	-40.6
CS069-1B	398.6	124.2	55.6	382.4	51.2	347	60	69.7
CS072-1A	415.5	437.1	-64.6	137.2	-26.3	347	60	-43.8
CS073-2B	419.0	431.3	64.7	373.7	25.1	347	60	59.3
CS075-2B	432.3	289.7	68.4	327.2	16.7	347	60	46.1
BM002-2A	437.5	435.1	65.6	372.3	33.3	344	54	64.4
BM003-1A	439.5	97.5	79.1	355.6	39.9	344	54	70.8
BM005-1A	446.0	167.6	79.0	341.4	46.9	344	54	69.8
BM006-1B	451.0	444.7	84.4	349.6	37.0	344	54	67.4

TABLE III | Continued

Site Nº	Stratigraphic level (m)	Geographic coordinates Dec. (º)	Geographic coordinates Inc. (º)	Stratigraphic coordinates Dec. (º)	Stratigraphic coordinates Inc. (º)	Dip az. (º)	Dip. (º)	VGP Lat. (º)
BM007-1B	454.5	112.4	85.0	347.7	39.1	344	54	68.0
BM008-1A	457.5	382.0	68.0	357.2	18.1	344	54	57.7
BM009-1A	458.5	108.4	80.2	353.3	41.3	344	54	71.4
BM010-1A	470.2	357.3	61.6	349.7	8.3	344	54	51.6
BM011-1C	478.0	395.8	75.8	355.4	26.8	344	54	62.4
MM001-1A	489.5	337.2	66.3	338.1	10.3	340	56	48.8
MM003-1A	501.2	437.3	73.0	359.3	34.8	340	56	67.7
MM004-1A	509.8	109.3	72.4	357.4	44.1	340	56	74.2
MM005-1A	519.0	283.1	46.0	303.6	4.4	340	56	26.1
MM006-1A	523.5	213.6	-43.7	195.1	-2.4	340	56	-47.5
MM006-2A	523.5	207.3	-83.5	164.3	-29.5	340	56	-61.0
MM007-2A	524.5	137.0	40.3	402.4	71.7	340	56	59.1
MM008-1B	536.0	320.9	80.4	335.5	24.8	340	56	54.4
MM008-2B	536.0	121.6	74.7	351.8	45.5	340	56	74.0
MM009-1A	536.2	371.9	62.1	353.8	9.8	340	56	53.0
MM010-1A	554.8	420.5	59.0	372.8	24.7	340	56	59.4
MM010-2A	554.8	329.7	57.6	333.9	1.9	340	56	43.1
MM011-1A	606.8	356.6	-58.7	138.4	-62.5	340	56	-59.7
MM013-1C	617.0	302.2	-64.6	183.4	-52.3	340	56	-81.0
MM014-2A	624.5	317.8	-64.8	174.7	-56.6	340	56	-84.0
MM015-2A	628.9	318.4	-59.8	179.8	-61.0	340	56	-89.4
MM016-1B	632.2	213.1	-59.2	184.0	-13.5	340	56	-55.2
MM017-1A	636.3	278.2	-68.6	184.0	-42.0	340	56	-72.4
MM018-1A	640.9	287.4	-57.8	197.6	-48.5	340	56	-71.4
MM019-1A	647.5	246.5	-78.4	172.6	-32.8	340	56	-65.5
MM020-1A	652.2	331.6	-71.2	162.5	-52.6	340	56	-73.8
MM021-1A	654.9	169.6	-57.3	164.6	-1.8	340	56	-47.1
MM025-1A	684.9	158.5	-24.6	158.5	31.4	340	56	-28.2
MM026-1B	688.3	246.4	88.2	336.6	34.1	340	56	59.7
MM027-1A	691.5	326.7	40.6	329.3	-14.6	340	56	33.6
MM027-2A	691.5	275.3	49.8	302.7	10.8	340	56	27.8
MM028-1A	703.5	189.1	82.1	333.4	40.7	340	56	61.3
MM029-1A	707.1	181.1	65.3	322.2	55.9	340	56	60.4
MM030-1A	713.0	120.0	76.5	350.4	44.0	340	56	72.4
MM030-1C	713.0	273.0	60.8	310.7	18.8	340	56	36.4
MM031-1B	714.8	285.8	87.0	335.9	32.2	340	56	58.3
MM032-1A	720.5	170.5	48.7	311.4	72.9	340	56	55.5
MM034-1A	728.9	310.4	28.0	311.7	-22.4	340	56	20.8
MM035-1B	730.3	142.5	62.1	353.9	60.1	340	56	85.4
La Tossa Section								
LT100-1A	875.3	376.0	56.8	351.5	30.9	320	35	64.1
LT101-1A	884.1	364.2	68.5	338.4	37.8	320	35	62.7
LT102-1A	893.8	408.3	65.4	357.5	47.8	320	35	77.2
LT103-2A	896.0	349.3	64.4	334.0	31.6	320	35	57.0
LT104-1A	901.3	380.3	61.2	350.5	35.7	320	35	66.8
LT105-1A	903.4	391.6	53.4	362.3	33.6	320	35	66.8
LT106-2A	906.0	359.3	67.3	337.2	35.8	320	35	61.0
LT107-2A	908.5	378.3	56.5	352.9	31.3	320	35	64.7
LT108-2B	911.3	367.2	53.0	358.2	30.0	340	25	64.5
LT109-2A	913.0	395.3	61.8	371.9	43.4	340	25	71.1
LT110-2A	916.0	374.1	59.3	360.7	37.1	340	25	69.2
LT111-1A	919.5	384.6	64.7	364.2	43.8	340	25	73.8
LT112-1A	922.9	366.6	61.2	355.6	37.8	340	25	69.4
LT113-1A	927.1	379.6	57.3	364.9	36.1	340	25	68.1
LT114-1A	931.8	393.6	58.3	373.1	39.9	340	25	68.2
LT115-2C	937.3	390.3	61.9	369.0	42.4	340	25	71.5
LT116-1A	941.8	381.7	49.9	369.2	29.5	340	25	63.1
LT117-1A	945.0	373.3	58.0	360.7	35.7	340	25	68.2
LT118-1A	948.0	348.4	54.0	345.4	29.2	340	25	61.2
LT119-1A	951.3	402.2	64.4	373.8	47.2	340	25	72.7
LT120-2B	955.5	372.5	63.3	358.2	40.6	340	25	71.6
LT121-2A	959.6	364.6	62.0	354.1	38.4	340	25	69.5
LT122-2A	964.7	368.5	60.1	357.0	37.0	340	25	69.0

TABLE III | Continued

Site Nº	Stratigraphic level (m)	Geographic coordinates Dec. (º)	Geographic coordinates Inc. (º)	Stratigraphic coordinates Dec. (º)	Stratigraphic coordinates Inc. (º)	Dip az. (º)	Dip. (º)	VGP Lat. (º)
LT123-2B	969.1	374.9	66.3	358.2	43.7	340	25	74.0
LT126-1B	979.8	428.8	49.1	402.9	43.0	340	25	51.0
LT127-1B	983.8	371.5	56.5	360.1	33.9	340	25	67.1
LT129-1A	1035.0	408.8	64.4	377.3	48.8	340	25	71.7
LT130-1B	1036.5	397.7	52.5	379.0	35.8	340	25	63.0
LT131-1A	1042.7	409.1	63.0	378.8	47.8	340	25	70.2
LT132-1B	1047.0	391.7	54.9	373.7	36.4	340	25	65.8
LT133-2A	1053.2	383.7	53.0	369.3	32.8	340	25	65.1
LT135-1A	1057.2	386.3	76.0	356.8	54.1	340	25	82.7
LT138-1A	1066.0	406.5	72.7	367.6	54.8	340	25	81.4
LT139-2A	1069.1	390.9	57.0	372.2	38.1	340	25	67.4
LT141-1A	1074.5	381.6	44.3	371.2	24.1	340	25	59.5
LT145-1B	1085.2	372.5	46.5	363.8	24.4	340	25	61.1
LT146-1A	1090.2	232.7	-61.4	202.1	-47.6	340	25	-67.9
LT147-1A	1092.7	207.3	-31.8	199.9	-13.7	340	25	-51.2
LT148-2A	1096.2	223.1	-54.3	201.5	-38.8	340	25	-63.3
LT150-1B	1102.5	212.0	-62.0	186.0	-41.4	340	25	-71.6
LT151-1A	1104.4	166.6	-47.6	164.6	-22.7	340	25	-57.4
LT152-1B	1107.7	122.8	-84.5	148.3	-71.2	339	14	-65.0
LT153-2B	1110.9	332.3	63.2	334.2	49.2	339	14	66.3
LT155-1B	1124.7	210.0	-45.5	201.5	-36.4	339	14	-62.0
LT159-1B	1129.2	213.0	-54.8	200.4	-45.5	339	14	-67.8
LT157-1A	1135.2	304.9	-49.1	292.2	-59.9	339	14	-12.6
LT158-2A	1140.2	380.7	43.3	373.8	32.4	339	14	63.3
LT160-1A	1199.5	325.5	56.4	329.8	36.8	340	20	57.0
LT161-1B	1202.0	365.6	63.0	355.6	44.3	340	20	74.1
LT163-1B	1208.3	369.8	45.5	363.0	27.6	340	20	63.0
LT164-1A	1212.0	343.4	72.2	341.3	52.2	340	20	72.9
LT165-1A	1214.7	380.5	63.1	364.8	46.2	340	20	75.5
LT166-1C	1219.7	393.4	45.6	381.3	32.1	340	20	59.8
LT167-1A	1223.0	428.5	68.1	388.5	60.5	340	20	68.8
LT001-2A	1225.8	336.4	57.7	340.0	48.1	355	10	69.6
LT168-2A	1226.0	383.7	45.2	373.9	29.6	340	20	61.7
LT002-1B	1230.3	330.1	56.9	334.9	47.6	355	10	66.0
LT003-1A	1232.2	379.7	62.7	373.6	53.5	355	10	76.9
LT004-2A	1236.0	375.2	64.9	369.7	55.4	355	10	80.6
LT005-1A	1237.5	377.7	60.0	372.5	50.7	355	10	75.8
LT006-2B	1239.1	328.7	19.3	329.8	10.3	355	10	44.8
LT007-2A	1241.4	381.2	24.2	379.6	15.2	355	10	52.0
LT008-1A	1243.8	371.4	63.9	367.0	54.3	355	10	81.3
LT009-1B	1246.1	381.6	61.9	375.2	52.7	355	10	75.4
LT010-1A	1248.1	340.1	72.5	345.1	62.7	355	10	78.8
LT011-1A	1251.6	364.6	51.0	362.9	41.1	355	10	71.9
LT012-1B	1253.3	352.8	28.7	352.9	18.7	355	10	57.5
LT013-1B	1257.3	356.7	59.8	356.2	49.8	355	10	78.7
LT014-1B	1261.3	360.9	46.9	359.9	36.9	355	10	69.1
LT015-1A	1263.3	287.7	76.0	314.2	69.9	355	10	57.4
LT016-1A	1266.6	353.9	67.2	354.0	57.2	355	10	84.1
LT017-1A	1272.6	349.9	67.7	349.9	67.7	0	0	78.5
LT018-1A	1273.6	381.6	65.7	381.6	65.7	0	0	73.4
LT019-1B	1273.8	359.0	66.1	359.0	66.1	0	0	83.0
LT020-1A	1275.8	342.2	56.5	342.2	56.5	0	0	75.6
LT021-1B	1277.7	304.2	63.6	304.2	63.6	0	0	50.1
LT023-1A	1288.8	351.5	19.0	351.5	19.0	320	25	57.4
LT024-1A	1292.1	110.5	-15.0	110.5	-15.0	320	25	-20.4
LT026-2A	1299.8	334.5	68.0	334.5	68.0	320	7	70.1
LT027-1A	1302.7	341.5	63.7	341.5	63.7	320	7	76.1
LT030-1B	1320.1	354.2	54.0	354.2	54.0	320	7	81.7
LT031-1A	1322.1	347.8	58.6	347.8	58.6	340	25	80.4
LT033-1A	1338.8	362.9	55.3	362.9	55.3	320	7	83.9
LT034-1B	1345.1	435.8	16.8	435.8	16.8	320	7	16.3